Direct reprogramming of human fibroblasts into insulin-producing cells by transcription factors

Running title: Reprogramming of fibroblasts to insulin-producing cells

Marta Fontcuberta-PiSunyer[1,2], Ainhoa García-Alamán[1,3], Èlia Prades[1], Noèlia Téllez[3,4,5], Hugo Figueiredo[1,2], Rebeca Fernandez-Ruiz[1,3], Sara Cervantes[1,3], Carlos Enrich[1,2], Laura Clua[6], Javier Ramón-Azcón[6], Christophe Broca[7], Anne Wojtusciszyn[7,8], Anna Novials[1,2], Nuria Montserrat[6,9,10], Josep Vidal[1,2,3,11], Ramon Gomis[1,2,3,12], Rosa Gasa[1,3 *]

[1] Institut d'Investigacions Biomèdiques August Pi i Sunyer (IDIBAPS), Barcelona, Spain

[2] Faculty of Medicine and Health Sciences, Universitat de Barcelona, Barcelona, Spain

[3] Centro de Investigación Biomédica en Red de Diabetes y Enfermedades Metabólicas Asociadas (CIBERDEM), Spain

[4]Institut d'Investigació Biomèdica de Bellvitge (IDIBELL), Barcelona, Spain

[5]Biosciences department, University of Vic - Central University of Catalonia (UVic-UCC), Vic, Spain

[6]Institute for Bioengineering of Catalonia (IBEC), The Barcelona Institute of Technology (BIST), Barcelona, Spain

[7]CHU Montpellier, Laboratory of Cell Therapy for Diabetes (LTCD), Hospital St-Eloi, Montpellier, France

[8]Service of Endocrinology, Diabetes and Metabolism, Lausanne University Hospital, Lausanne, Switzerland

[9]Centro de Investigación Biomédica en Red en Bioingeniería, Biomateriales y Nanomedicina, Madrid, Spain

[10]Catalan Institution for Research and Advanced Studies (ICREA), Barcelona, Spain

[11]Endocrinology and Nutrition Department, Hospital Clinic of Barcelona, Barcelona, Spain

[12]Universitat Oberta de Catalunya (UOC), Barcelona

*corresponding author and lead contact

rgasa@clinic.cat

ABSTRACT

Direct lineage reprogramming of one somatic cell into another bypassing an intermediate pluripotent state has emerged as an alternative to embryonic or induced pluripotent stem cell differentiation to generate clinically relevant cell types. One cell type of clinical interest is the pancreatic β cell that secretes insulin and whose loss and/or dysfunction leads to diabetes. Generation of functional β-like cells from developmentally related somatic cell types (pancreas, liver, gut) has been achieved via enforced expression of defined sets of transcription factors. However, clinical applicability of these findings is challenging because the starting cell types are not easily obtainable. Skin fibroblasts are accessible and easily manipulated cells that could be a better option, but available studies indicate that their competence to give rise to β cells through similar direct reprogramming approaches is limited. Here, using human skin fibroblasts and a protocol that ensures high and consistent expression of adenovirus-encoded reprogramming factors, we show that the transcription factor cocktail consisting of Pdx1, Ngn3, MafA, Pax4 and Nkx2-2 activates key β cell genes and down-regulates the fibroblast transcriptional program. The converted cells produce insulin and exhibit intracellular calcium responses to glucose and/or membrane depolarization. Furthermore, they secrete insulin in response to glucose *in vitro* and after transplantation *in vivo*. These findings demonstrate that transcription factor-mediated direct reprogramming of human fibroblasts is a feasible strategy to generate insulin-producing cells.

INTRODUCTION

The discovery that adult somatic cells can be reprogrammed into induced pluripotent stem cells (iPSC) [1, 2] has revolutionized current biological and medical research. Human iPSC can provide valuable platforms for drug and toxicology screens, for investigating human development and for disease modeling. Furthermore, the possibility of differentiating iPSC into clinically relevant cell types for autologous cell therapy has pushed the field of regenerative medicine forward. However, current iPSC technology is still technically demanding, expensive, time consuming and produces cells of variable quality. Similarly, design of the *in vitro* differentiation protocols to generate specific cell types is not trivial. Recapitulation of in vivo developmental pathways using signaling molecules is considered the most effective approach, but defining and adjusting proper in vitro differentiation conditions is not a straightforward task, and differentiation protocols are often long and expensive, present poor reproducibility and have variable efficiencies among laboratories.

An alternative strategy to produce cell types of interest is direct lineage reprogramming, which entails the direct conversion of one differentiated cell type into another bypassing an intermediate pluripotent stage. This strategy is often based on the forced expression of cocktails of transcription factors (TF) that normally function as potent fate determinants of the cell type of interest in development [3-5]. This approach presents several advantages over pluripotent cell derivation including its relative simplicity and speed (fewer induction steps) and, in terms of translational potential, its safety due to avoidance of the tumorigenic risk associated with pluripotency [6]. Moreover, as with iPSC, this strategy allows autologous transplantation thus eluding the problem of allograft rejection.

Pancreatic beta (β) cells produce insulin, which controls whole body glucose

98 homeostasis. Relative or complete deficit of functioning β cells is a hallmark of diabetes
99 and thus β-cell replacement has emerged as a promising therapeutic approach to treat
100 and eventually cure this disease. To date, derivation of β-cells from pluripotent
101 (embryonic and iPS) cells has been intensively studied, with significant progress made
102 during the past fifteen years [7-11]. Yet, current protocols are still on the way of
103 standardization and face important challenges including low number and functional
104 maturation of generated β-like cells [12, 13]. Direct lineage reprogramming strategies to
105 create β-cells bypassing the iPSC stage have also been explored. In this line, the
106 Melton laboratory developed the first TF-based *in situ* conversion of mouse pancreatic
107 exocrine cells towards insulin-producing cells through expression of three TFs: Pdx1,
108 Ngn3 and MafA (hereafter PNM)[14]. Subsequently, these factors, individually or
109 combined, have been shown to promote β-cell-like features in related endodermal cell
110 lineages such as pancreatic ductal cells, hepatic, intestinal or stomach cells [15-21].
111
112 One central aspect in direct reprogramming approaches, particularly when considering
113 their clinical applicability, is the choice of cell source. Ideally, the starting material
114 should be accessible, easy to handle/grow and susceptible to reprogramming. To date
115 fibroblasts, which can be readily obtained from small skin biopsies, are commonly used
116 as cell source for IPSC generation. Remarkably, they have also been directly
117 reprogrammed towards somatic cell types including cardiomyocytes [22], chondrocytes[23],
118 neurons [24] or oligodendrocyte progenitors [25]. In the pancreas field, human fibroblasts
119 have been converted into expandable pancreatic progenitor populations through
120 transient overexpression of iPSC factors in conjunction with lineage-determining
121 soluble factors [26] and into insulin-producing cells following long protocols that are
122 reminiscent of the small molecule-based directed differentiation procedures applied to
123 stem cells [26-28]. However, attempts to use cell-specific TFs to directly transform
124 fibroblasts into β cells have yielded discouraging results [14, 20, 29, 30].
125

The growing potential of direct lineage reprogramming to generate specialized cell types, the medical interest in pancreatic β cells and the prevailing challenges for the generation of these cells via conventional directed differentiation from pluripotent cells, prompted us to examine the amenability of fibroblasts to be reprogrammed to β cells using cell-specific transcription factors in a more comprehensive manner. Here we show that the combination of five endocrine TF induces activation of the β-cell transcriptional program in human fibroblasts. Furthermore, we show that reprogrammed fibroblasts produce and secrete insulin *in vitro* and *in vivo*. We believe these findings demonstrate the feasibility of this approach and set the basis to explore this path for generation of insulin-producing cells for disease modeling and cellular therapy.

MATERIALS and METHODS

Fibroblasts

Human foreskin fibroblasts were prepared from a foreskin biopsy from a 3-year old individual after obtaining his parents' written informed consent (HFF1). Adult human dermal fibroblasts were prepared from arm biopsies of two T1D individuals after obtaining their written informed consent (HDF-DT1-1, HDF-DT1-2). In brief, skin samples were collected in sterile saline solution, divided into small pieces, and allowed to attach to cell culture dishes before adding Iscove's modified Dulbecco's medium (Invitrogen, Carlsbad, CA, USA) supplemented with 10% human serum (Sigma, St. Louis, MO, USA) and penicillin/streptomycin (0.5X) (Invitrogen). After 10 days of culture at 37°C, 5% CO2, fibroblast outgrowths were dissociated and split 1:4 using a recombinant trypsin-like enzyme (TrypLE Select, Invitrogen). Additional fibroblast preparations were commercially available: HFF2 (SCRC1041^{TM}, ATCC, Manassas, VA, USA) and HDF-1 (PCS-201-012, ATCC) and HDF-2 (Cell Applications, San Diego, CA, USA).

154

155 **Human islets**

156 Human islets were prepared by collagenase digestion followed by density gradient
157 purification at the Laboratory of Cell Therapy for Diabetes (Hospital Saint-Eloi,
158 Montpellier, France), as previously described [31]. After reception in Barcelona, human
159 islets were maintained in culture for 1-3 days in RPMI-1640 with 5.5mM glucose, 10%
160 fetal bovine serum (FBS) and antibiotics, before performing the experiments.
161 Experiments were performed in agreement with the local ethic committee (CHU,
162 Montpellier) and the institutional ethical committee of the French Agence de la
163 Biomédecine (DC Nos. 2014-2473 and 2016-2716). Informed consent was obtained for
164 all donors.

165

166 **Recombinant adenoviruses**

167 The adenoviral expression vector pAd/CMV/V5-DEST carrying mouse Pdx1, Ngn3,
168 MafA and 2A-Cherry under the CMV promoter was kindly provided by Dr. Q. Zhou,
169 Harvard University[29]. The recombinant adenovirus (termed Ad-PNM) was generated
170 after Pac1 digestion and transfection into HEK293 cells. The recombinant adenovirus
171 encoding Pdx1 was kindly provided by the Beta Cell Biology Consortium. The
172 recombinant adenovirus encoding MafA was purchased from Vector Biolabs (Chicago,
173 IL, USA). All other recombinant adenoviruses encoding single transcription factors
174 (Ngn3, NeuroD1, Nkx2.2, Nkx6.1 and Pax4) were described previously[18, 32].

175

176 **Reprogramming protocol**

177 Fibroblasts were grown in DMEM media supplemented with 10% (v/v) fetal bovine
178 serum (FBS), 100 U/ml penicillin, 100 µg/ml streptomycin and 1% Glutamax. They
179 were plated onto 96-well plates (9 500 cells per well) for MTT and BrdU assays, onto
180 12-well plates ($1.25x10^5$ cells/well) for gene expression, insulin secretion,
181 immunofluorescence and caspase assays and onto 10 cm plates ($1.5x10^6$ cells/plate)

for transplantation experiments. Infection with Ad-PNM was performed when fibroblasts reached 80% confluence, normally 1-2 days after seeding. In brief, for 12-well plates, fibroblasts were incubated with 0.6ml complete culture medium containing Ad-PNM at a dose of 15 moi (multiplicity of infection) for 16-20 h. After virus removal, media was changed to RPMI-1640 medium containing 6% FBS and antibiotics. Two and five days after incubation with Ad-PNM, fibroblasts were infected for 6-8 h with Ad-Pax4 (50 moi) and Ad-Nkx2.2 (50 moi) respectively. The transfection reagent Superfect (Qiagen, Venlo, Netherlands) was always added to the virus-containing media in order to achieve efficient adenoviral infection and transgene expression in fibroblasts. Amounts were scaled down or up according to the well size. To prepare spheroids, one day after Ad-Nkx2.2 infection, cells were trypsinized and transferred (1 200-1 800 cells/ well) to 96-well Nunclon Sphera plates (Thermo Scientific) for gene expression, immunofluorescence and insulin secretion assays. Cell spheroids (1 000 cells/cluster) for transplantation were generated in AggreWell plates (StemCell Technologies, Saint Égrève, France**)**

RNA isolation and reverse transcriptase polymerase chain reaction (RT-PCR)

Total RNA from cultured cells was isolated using NucleoSpin®RNA (Macherey-Nagel), Düren, Germany) following the manufacturer's manual. Total RNA from enucleated eyes was extracted using Trizol reagent (Sigma) and then cleaned and DNAse-treated using RNeasy mini columns (Qiagen) prior to cDNA synthesis. First-strand cDNA was prepared using Superscript III Reverse Transcriptase (Invitrogen) and random hexamers in a total volume of 20 ul and 1/40 to 1/200 of the resulting cDNA was used as a template for real time PCR reactions. Real time PCR was performed on an ABI Prism 7900 detection system using Gotaq master mix (Promega, Madison, WI, USA). Expression relative to the housekeeping gene *TBP* was calculated using the delta(d)Ct method and expressed as 2^(-dCT) unless otherwise indicated. Primer sequences are provided in Table S3.

BrdU and MTT assays

For quantification of cell proliferation, cells in 96-well plates were cultured overnight with medium containing 5-bromo-2'-deoxuridine (BrdU). BrdU incorporation was determined colorimetrically with the Cell proliferation ELISA kit (Roche, Basilea, Switzerland) following the manufacturer's instructions. For assessing cell viability, cells grown in 96-well plates were incubated with medium containing 0.75 mg/ml of 3-(4,5-dimethythiazol-2-yl)-2,5-diphenyltetrazolium bromide (MTT) for 3 hours at 37ºC. The resulting formazan crystals were solubilized in Isopropanol/0.04 N HCl solution and optical density [1] was read at 575 nm and 650 nm using a Synergy HT reader (BIO-TEK Instruments, Winooski, VT, USA). The OD (575-650) was expressed relative to control fibroblasts, which were given the value of 100%.

Calcium imaging

To study glucose-dependent calcium influx, cells were washed with Hanks' Balanced Salt Solution (HBSS, Sigma) and incubated with Fluo4-AM (Life Technologies) in fresh 2.5 mM glucose Krebs-Ringer bicarbonate buffer for 1 hour at 37ºC in the dark. Intracellular calcium fluorescence was recorded from fluo-4-loaded cells using a Leica TCS SPE confocal microscope with an incubation chamber set at 37C, and a 40x oil immersion objective. Fluorescent images and average fluorescence intensity were acquired at 600Hz every 1.8 seconds, using a 488nm excitation laser, an emission set at 520 with a bandwidth of 10nm. Image registry consisted of: 5 min in 2 mM glucose-Krb buffer, 10 min in 22 mM glucose-Krb buffer and 5 min in 30 mM KCl-Krb buffer. Average fluorescence intensity images of each individual cell were analyzed with LAS AF Lite and Fuji programs.

In vitro glucose-induced insulin secretion and content

Cells in 2D or 3D aggregates were washed with phosphate-buffered saline (PBS) and preincubated for 30-45 min at 37°C in Hepes-buffered Krebs-Ringer buffer with 2mM glucose. Preincubation solution was then removed and cells incubated with the same buffer containing different glucose concentrations glucose for additional 90 min. Supernatants were collected to measure secreted insulin or C-peptide. Cells were lysed in detergent-containing buffer (Tris-HCl pH8 50mM, NaCl 150mM, SDS 0.1% (w/v), Igepal CA-630 1%, Na deoxycholate 0.5%) to determine C-peptide content. Human insulin was measured using a human Insulin ELISA kit (Crystal Chem, Zaandam, Netherlands) and C-peptide using a human C-peptide ELISA kit (Mercodia, Uppsala, Sweden).

Electron microscopy

Cell spheroids were collected, washed with PBS and fixed with 4% paraformaldehyde/ 0.5% glutaraldehyde (Sigma) mixture in 0.1M phosphate buffer (PB) pH7.4 for 30min at 4°C and gentle agitation. Cells were then transferred to fresh fixation solution and maintained at 4°C until secondarily fixed with 1% uranyl acetate and 1% osmium tetroxide. Cells were then dehydrated, embedded in Spurr's Resin and sectioned using Leica ultramicrotome (Leica Microsystems). Conventional transmission electron microscopy (TEM) images were acquired from thin sections using a JEOL-1010 electron microscopy equipped with an SC1000 ORIUS-CCD digital camara (Gatan).

Transplant procedures

Adult (12-20 week old) immunocompromised NSG-SCID mice (005557, Jackson Laboratories) received implants in the anterior chamber of the eye (ACE), subcutaneously or between the omental sheets as previously described[33, 34]. A total of 150-200 human islets, 300 iβ-like cell or HFF1 spheroids (1 200-1 800 cells/cluster) were transplanted per eye and approximately 4000-iβ-like cell spheroids (750-1 000 cells/cluster) were transplanted into either of the other two implant sites. For

subcutaneous and omental transplants, collagen scaffolds were used. Briefly, the cell-laden collagen hydrogel was prepared by mixing 150 µl of a 4 mg/ml rat tail type I collagen (Corning, NY, USA) solution, prepared following the manufacturer's instructions, with iβ-like cell clusters (pelleted by gentle centrifugation) and poured onto a cylindrical 8 mm diameter x 1 mm thick PDMS mold (Dow Corning Sylgard 184 Silicone Elastomer). The hydrogel was polymerized for 20 min at 37 ºC, detached from the mould and maintained in tissue culture dishes with warm RPMI-1640 medium until transplant (usually 2-3 hours). Constructs were introduced in the abdominal subcutaneous space through a small (1–2 mm) incision. Alternatively, constructs were placed on the omentum close to the duodenal-stomack junction and fixed using Histoacryl translucent (Braun, Kronberg im Taurus, Germany). The local ethical committee for animal experimentation of the University of Barcelona approved all animal experiments and procedures.

Graft viability and function analysis

To assess vascularization and cell viability in ACE implants, iβ-like clusters were labeled with the long-term tracer for viable cells CFDA (Invitrogen) before transplantation. At day 10 post-transplantation, mice received an intravenous injection of RITC-dextran and in vivo imaging was used to assess functional vascularization and cell viability [34]. For determination of glucose-induced insulin secretion, mice were fasted for 5-6 h and then injected intraperitoneally with glucose (3g/Kg). Aqueous humor from mice with ACE implants was obtained 30 minutes after the glucose challenge and kept frozen until human insulin determination. Tail blood before and after (20 minutes) the glucose challenge was obtained from mice with subcutaneous and omental implants. Human insulin in aqueous humor and in plasma was determined using an ultrasensitive Human Insulin ELISA (Chrystal Chem).

Immunofluorescence

293 iβ-like cells grown in 2D were fixed with 4% (v/v) paraformaldehyde (PFA) during 15
294 min and incubated with blocking solution (0.25% (v/v) Triton, 6% (v/v) donkey serum,
295 5% (w/v) BSA in PBS for 1 h at room temperature. Slides were then incubated with
296 primary antibodies diluted in PBS-triton 0.1% (v/v) containing 1% donkey serum
297 overnight at 4 o C. iβ-like cells grown in spheroids were fixed with 4% (v/v)
298 paraformaldehyde (PFA) for 15 min at 4ºC, permeabilized with 0.5% (v/v) Triton in PBS
299 for 20 min and blocked with 0.5% (v/v) Triton/ FBS 10% (v/v) in PBS during 1 h at room
300 temperature. Slides were then incubated with primary antibodies diluted in blocking
301 solution overnight at 4^{o}C. Eyes were obtained by enucleation, fixed overnight in 2%
302 (v/v) PFA, dehydrated with ethanol gradient, cleared with xylene and paraffin-
303 embedded. 3-µm thick eye sections were used for standard immunofluorescence
304 staining protocol. Images were acquired in a Leica DMR HC epifluorescence
305 microscope (Leica Microsystems).
306 Primary antibodies used were: Insulin (DAKO, 1:400), C-peptide (Abcam, 1: 200 or
307 Hybridoma Bank; 1:40), vimentin (Sigma, 1:200), HLA (Abcam, 1:100), Nkx-2.2
308 (Hybridoma Bank, 1:400), Pdx1 (Abcam 1:500) and MafA (Novus Biologicals 1:75).
309 The antigen-primary antibody immune complex was visualized with secondary
310 antibodies conjugated to Alexa Fluor 488 (Jackson Immunoresearch, 1:250), Alexa
311 fluor 555 (Molecular Probes, 1:400) or Alexa fluor 647 (Jackson Immunoreserach,
312 1:250). Cell nuclei were counterstained with Hoescht (SIGMA, 1:500). Representative
313 images were taken using a confocal microscope (LEICA TCS SPE).
314

315 **Statistical analysis**

316 Data are presented as mean ± standard error of the mean (SEM) from at least three
317 independent reprogramming experiments, with one to four biological replicates per
318 experiment. Significant differences between the means were analyzed by the two-tailed
319 unpaired Student's *t*-test, one sample t-test or one-way ANOVA followed by Tukey's
320 multiple comparison tests as indicated in the figure legends. Statistical analysis was

performed with GraphPad Prism 8.00 and Microsoft Office Excel 2007 and differences were considered significant at $p<0.05$. No methods were used to determine whether the data met assumptions of the statistical approach (e.g. test for normal distribution).

RESULTS

Introduction of the transcription factors Pdx1, Ngn3 and MafA (PNM) leads to activation of β-cell genes and insulin production by human fibroblasts.

We first investigated whether human fibroblasts could be directly converted towards the β-cell lineage through exogenous expression of the PNM factors Pdx1, Neurog3 and MafA. As delivery method we used a polycistronic adenoviral vector encoding the three transcription factors and a Cherry reporter protein (Ad-PNM hereafter) that had been previously used in the reprogramming of pancreatic acinar cells towards islet cells [35]. We chose adenoviruses for transgene delivery because they allow high expression of transgenic proteins and, most importantly, don't integrate in the host genome. However, we couldn't detect Cherry immunofluorescence after viral treatment of human fibroblasts (Fig. S1), which was in agreement with other reports showing poor adenoviral transduction efficiency in fibroblastic cells [36, 37]. In an attempt to boost adenoviral transduction, we added an activated dendrimer normally used in transfections to the virus-containing media and, in stark contrast to Ad-PNM alone, we observed abundant (>80%) fibroblasts that were Cherry$^+$ three days after exposure to the virus+dendrimer (Fig.S1 and Fig.1A). Interestingly, Cherry$^+$ cells were still readily visible 7 days post-viral treatment (Fig. 1A). Likewise, transcripts encoding the PNM factors were detected at 3 and 7 days after viral treatment (Fig.1B). Remarkably, three days after addition of Ad-PNM we detected low levels of *INS* transcripts that were dramatically increased by day 7 (Fig.1C). We examined the influence of distinct culture media on *INS* mRNA levels and found that cells cultured in RPMI-1640 supplemented

with 6% FBS exhibited the highest degree of *INS* gene activation relative to cells cultured in DMEM or CMRL-1066, reaching values that were 900-fold lower than human islets but similar to those attained in directed differentiation protocols from iPSC [38] (Fig. 1D). The PNM factors also induced moderate levels of several endocrine transcription factor genes including *NEUROD1*, *INSM1, PAX4*, *NKX2-2* and *ARX*, although they did not induce the key β-cell TF *NKX6-1* (Fig.1E). Unexpectedly, the PNM factors also induced the islet hormone genes *GLUCAGON (GCG)* and *SOMATOSTATIN (SST)*, albeit to levels less than those observed for *INS (*as indicated by lower expression relative to the housekeeping gene *TATA BINDING PROTEIN,* (*TBP*) (Fig. 1F). Conversely, PNM down-regulated the expression of genes associated with fibroblast signature, including several factors involved in maintenance of the fibroblastic transcriptional program such as *TWIST2*, *PRRX1* and *LHX9* [39] (Fig. 1G). Together, these experiments show that the PNM factors induce a transcriptional switch from a fibroblastic towards an endocrine program in human fibroblasts.

Addition of Pax4 and Nkx2-2 to the PNM factors improves reprogramming of human fibroblasts towards the β-cell lineage.

Due to the suboptimal conversion of fibroblasts into β-like cells using the PNM factors (i.e. as reflected by the lack of induction of *NKX6-1* mRNA and the expression of other endocrine hormones), we tested the effects of adding other transcription factors to the reprogramming cocktail, namely Nkx6-1, Pax4, NeuroD1 and Nkx2-2. Among all tested combinations, we found that expression of PNM in a single polycistronic adenovirus followed by sequential expression of Pax4 and Nkx2-2 (hereafter this combination is named 5TF) resulted, ten days after initial PNM infection, in the highest degree of *INS* gene activation accompanied by the blockade of *GCG* gene induction (Fig. 2A&B and Fig.S2). Moreover, 5TF reprogramming resulted in activation of *NKX6.1* and of the pan-endocrine factor *PAX6 genes (*Fig. 2B*).* At day 10, reprogrammed cells displayed an epithelial morphology (Fig. 2C) and hadn't grown as much as untreated fibroblasts

(day 10; 5TF: $44x10^3 \pm 3x10^3$ cells/well; control: $238x10^3 \pm 18x10^3$ cells/well, n=18). In fact, reprogrammed cells showed diminished proliferation as early as one day after PNM introduction, while remaining viable, as indicated by their retained ability to reduce MTT, similar to that of fibroblasts (Fig. 2D&E). At day 10, reprogrammed cells exhibited lower MTT reduction activity, likely due to their decreased cell numbers (Fig. 2E).

Consistent with the gene expression data, insulin protein was detected by immunofluorescence staining in both PNM and 5TF cells, being staining more robust in 5TF cells than in PNM cells (Fig. 2F). By contrast, neither glucagon nor somatostatin proteins were detected in either PNM or 5TF cells. We quantified the immunofluorescence images and found that 67.9±6.2% of cells in the culture were INS+ at day 10. The presence of endogenous insulin production was further confirmed by immunofluorescence staining using an antibody against C-peptide (Fig.2G) and by determining C-peptide content with an ELISA (control: 0.34 ± 0.14 pg/10^5 cells, n=9; 5TF: 16.06 ± 2.55 pg/10^5cells, n=16). To further establish the extent of reprogramming achieved with 5TF as compared to PNM, we studied expression of additional endocrine genes at day 10. We found that transcripts of β-cell differentiation TFs (i.e. *NEUROD1*, *INSM1*, *HNF1B, MAFB*), as well as some of the reprogramming TFs (*PDX1*, *NEUROG3*, *NKX2-2*) were higher in 5TF as compared to PNM (Fig. 3A). On the other hand, several genes associated with a mature β-cell phenotype were more upregulated by 5TF than PNM (*PCSK1*, *ABCC8*, *KCNJ11, GLP1R, GIPR, NCAM1, CXCR4*), whilst others (*CHGB*, *PTPRN*, *CX36*) were induced to similar extents by both TF combinations (Fig. 3B). In line with loss of *GCG* activation, the pro-convertase gene *PCSK2*, which is expressed at higher levels in α than β cells [40], was reduced by 5TF as compared to PNM (Fig.3B), supporting that sequential introduction of Pax4 and Nkx2-2 after PNM endorses the β-cell differentiation program in human fibroblasts. It should be noted that expression levels of the induced genes were lower than in human islets, with

differences ranging from 2-fold for *NCAM1* to 20,000-fold for *CHGB* (Fig. 3A,B, Table S1). Gene activation was sustained for at least eleven additional days under the same culture conditions despite declined expression of the reprogramming factor transgenes. Moreover, expression of some genes increased with time in culture (i.e. *NKX6.1, INSM1, ABCC8, CHGB*) (Fig.S3).

Lastly, we looked into genes that are selectively repressed (disallowed) in β cells [41]. In response to 5TF, several β-cell disallowed genes were significantly downregulated reaching expression levels comparable to human islets (*OAT*, *SMAD3*, *PDGFRA*, *CXCL12*, *LDHA*), while others remained unchanged (*REST*, I*GFBP4*). Among the studied genes only *MCT1* was induced by 5FT relative to parental HFF1 cells (Fig.3C).

Together, these results reveal that 5TF induces a transcriptional switch from a fibroblastic to a β-like cell identity that entails both selective gene activation and repression events. Hereafter, we will refer to cells generated following the 5TF protocol as induced β-like (iβ-like) cells.

In vitro assessment of human fibroblast-derived iβ-like cells.

Glucose-induced insulin secretion (GSIS) by β cells is mediated by glucose metabolism, closure of ATP-dependent potassium channels, membrane depolarization and opening of voltage-dependent calcium channels, resulting in an increase in cytosolic Ca^{2+} that triggers insulin exocytosis. We investigated whether iβ-like cells exhibited β-cell functional features *in vitro* and begun by determining their ability to increase intracellular Ca^{2+} in response to glucose and membrane depolarization elicited by high potassium. We found that 65% of the cells exhibited a response to glucose, high potassium, or both whilst 35% of cells were unresponsive to either stimulus (Fig. 4A and video S1). Parental HFF1 cells not engineered for 5TF expression were universally unresponsive to these stimuli (Fig. 4B and video S2). Among responsive cells, approximately half responded to both glucose and high potassium and half

427 responded only to potassium (Fig. 4A). We observed heterogeneity in the amplitude
428 and kinetics of responses among individual cells (Fig. 4C). Next, we performed static
429 incubation assays to study glucose-induced insulin secretion (GSIS) and found that iβ-
430 like cells released similar amounts of human insulin at low (2mM) and high (20mM)
431 glucose concentrations (Fig.4D). Thus, at this stage, iβ-like cells lack a key signature
432 feature of normal β-cells, the ability to increase insulin secretion in response to
433 changes in extracellular glucose.

434 The differentiation and functionality of many cell types vary dramatically between three-
435 dimensional (3D) and two-dimensional (2D) monolayer cultures, the former being
436 closer to the natural 3D microenvironment of cells in a living organism. Considering
437 this, we reasoned that moving from the planar cell culture to a 3D system grown in
438 suspension might improve the functionality of iβ-like cells. To test this, we generated
439 spheroids of 1 200-1 800 iβ-like cells (average diameter of spheroids were 128±27 μm)
440 one day after introduction of Nkx2-2 and maintained them in culture for three additional
441 days (Fig.5A). Insulin protein was readily detected by immunostaining (Fig. 5B).
442 Further, iβ-like cell spheroids presented higher transcript levels for several β-cell
443 maturation markers including *INS*, the prohormone convertase *PCSK1*, and the ATP-
444 dependent potassium channel subunits *KCNJ11* and *ABCC8*, as compared to iβ-like
445 cells maintained in 2D cultures (Fig.5C). Consequently, the differences in expression
446 levels with human islets were reduced (Table S2). Consistent with improved
447 maturation; iβ-like cell spheroids exhibited a moderate but significant insulin secretory
448 response to glucose (fold 20mM/2mM: 2.02±0.18) as compared to 2D cultures (fold
449 20mM/2mM: 1.08-±0.15) in static GSIS assays (Fig. 5D,E). Similar results were
450 obtained using a different preparation of human foreskin fibroblasts (Fig. S4).
451 Therefore, three-dimensional culture during the last stage of the 5TF reprogramming
452 protocol (note that total length of the protocol remained unchanged) improved iβ-like
453 cell function

To establish the glucose threshold for stimulation of insulin secretion, iβ-like cell clusters were subjected to either 2,5,11 or 20mM glucose. Although there was some variability, when moved from 2mM to 5mM glucose, cells did not show a statistical significant increase in insulin secretion (Fig. 5F). They increased insulin secretion on average by a factor of 2.3 when moved from 2mM to 11mM or to 20mM glucose (Fig. 5F). These observations indicate that iβ-like cells are stimulated at higher glucose threshold. Remarkably, this concentration dependence of insulin secretion is similar to human islets that have a threshold at 3mM and a maximal response at 15mM [39]. In light of these results, we asked whether iβ-like cells presented recognizable secretory granules. Therefore, iβ-like cell clusters where fixed and prepared for conventional electron microscopy. The presence of multiple spherical electron-dense prototypical secretory vesicles was evident in most cells (Fig. 5G). These vesicles showed a high degree of morphological heterogeneity, presumably as consequence of their degree of maturation and/or loading. Although they did not have the appearance of typical insulin-containing granules from primary β cells, which are characterized by a clear halo surrounding a dark polygonal dense core [42], some of the vesicles exhibited a grey or less electron dense halo and looked similar to the granules described in insulin-positive cells generated from stem cells in original differentiation protocols [10, 43].

In vivo assessment of human fibroblast-derived iβ-like cells.

Lastly, we studied the maintenance of cellular reprogramming in vivo. To this end, we transplanted 300 iβ-like cell spheroids (1000 cells/spheroid) into the anterior chamber of the eye (ACE) of immune-deficient NOD *scid* gamma (NSG) mice (Fig. 6A,B). The ACE allows fast engraftment [44] and *in vivo* imaging[45]. To assess *in vivo* graft revascularization we used two-photon microscopy after injection of RITC-dextran and confirmed the presence of functional vessels in the grafts 10 days after transplantation

(Fig. 6C and video S1). We also established that the transplanted cells were viable by visualizing fluorescence of the long-term tracer CFDA (Fig. 6C). We then investigated whether reprogramming was retained in vivo. We first studied human *INS* gene expression in eye grafts harvested ten days after transplantation. As shown in Figure 6D, human *INS* transcripts were readily detectable and levels (expressed relative to *TBP*) were similar to those exhibited by iβ-like cells prior to transplantation (Fig.2A, Fig. 5C). Corroborating this result, there were abundant HLA+ (human cell marker) cells that stained for C-peptide and for the transcription factors PDX1, NKX2-2 and MAFA, which are produced from both viral transgenes and cellular genes, in the eye grafts (Fig. 6E and Fig. S5). Of the total number of HLA+ cells counted, 43.5±2.7% were also positive for C-peptide (Fig. 6F). In addition, thirty minutes after an intra-peritoneal glucose injection, human insulin was readily detectable in the aqueous humor of the eyes carrying iβ-like cell grafts (17 of 17, ranging from 11 to 158 mU/L), whereas no insulin was detected in eyes transplanted with non-engineered fibroblast clusters or in mice that received no transplants (Fig.6G). Average insulin levels achieved with 300 iβ-like cells were around 10-fold lower than those observed with 150-200 human islets (53±11 mU/L as compared to 688±99mU/L) (Fig. 6G). Together, these data confirm that cellular reprogramming persisted after transplantation.

Finally, to evaluate iβ-like cell function in vivo, approximately 4000 spheroids were loaded onto a collagen disk and deposited subcutaneously into the abdominal cavity of adult NSG mice. We detected low levels of circulating human insulin after a glucose challenge in 3 (of 3) and 2 (of 3) mice at days 15 and 30 post-transplantation, respectively (Fig. 6H). We repeated this experiment using the well-vascularized omentum as implant site and observed overall higher human insulin levels and significant glucose-stimulated insulin secretion at day 30 post-transplantation in 3 (of 3) mice (Fig. 6H). Together, these results demonstrate that iβ-like cells exhibit glucose-induced insulin secretion in vivo. Remarkably, glucose-induced plasma human insulin

levels observed in mice transplanted with 4000 iβ-like cell spheroids were in the same order of magnitude than mice transplanted with a total of 300-500 human islets into the ACE (Fig. 6H). Thus, correlating with determinations in the aqueous humor, these results reveal that iβ-like cell clusters secrete *in vivo* approximately one tenth of the amount of insulin released by human islets.

DISCUSSION

In this study, we have developed a 10-day long protocol to produce insulin-producing cells from human fibroblasts through sequential introduction of five lineage-determining transcription factors. Enforced expression of PNM+Pax4+Nkx2-2 results in concomitant activation of the β-cell and down-regulation of the fibroblastic transcriptional programs. Significantly, reprogrammed cells exhibit a functional β-cell like phenotype as judged by their expression of critical β-cell function genes and their ability to mobilize calcium and secrete insulin upon glucose stimulation. These findings warrant further investigations on TF-based reprogramming strategies to generate β-like cells from human fibroblasts.

When compared to other published TF-based reprogramming examples, iβ-like cells exhibited *INS* transcript levels similar to those of reprogrammed human pancreatic duct cells [20] and remarkably higher than those reached in human hepatocytes [46]. Still, expression levels of insulin and of other β-cell marker genes were lower than in human islets. Likewise, glucose-induced insulin secretion was modest, especially in terms of the amount of hormone secreted. We expect further progress by redefining culture conditions as it has been done in stem cell derivation protocols for more than a decade [7, 10, 43, 47-52]. For example here we report that, by merely moving from 2D to a 3D culture system, iβ-like cells acquired the ability to secrete insulin in response to glucose. Another simple strategy to improve the functionality of iβ-like cells would be the addition of soluble factors during or after introduction of the conversion TFs [38, 53, 54]. Some of these factors might be selected from the growing body of information on

molecules that enhance maturation of β cells generated from stem cells [55]. Interestingly, it has been shown that soluble molecules can even substitute the function of exogenous factors in some reprogramming protocols [56-58].

The use of skin fibroblasts as cell source in place of other less accessible cell lineages can facilitate clinical translation of this approach. Furthermore, the prospect of auto-transplantation and the avoidance of tumor-related concerns linked to pluripotent cell states are two additional assets of this type of direct reprogramming approaches. Here we show that iβ-like cell grafts are efficiently re-vascularized, viable and exhibit glucose-induced insulin secretion in vivo. Circulating human insulin levels in mice transplanted with iβ-like cells were lower but not far-off from those reported in publications using stem cell-derived insulin-producing cells (Table S2). Together, these results provide the foundation for further work aimed at evaluating the long-term function of transplanted iβ-like cell spheroids under pathophysiological contexts. It will be interesting to assess whether the in vivo environment aids in the maturation process of iβ-like cells as it has been reported for stem cell-derived β cell progenitors [49, 52].

In summary, our results demonstrate that it is possible to generate insulin-producing cells from human fibroblasts using lineage specific transcription factors. This work evidences the feasibility of direct lineage reprogramming to generate β-like cells from developmentally distant cell lineages. The relative technical simplicity and speed of this procedure together with the opportunity to generate patient-specific β cells for disease modeling and/or autologous transplantation warrants a more comprehensive evaluation of this approach in the future.

ACKNOWLEDGEMENTS

We are indebted to Lidia Sanchez, Yaiza Esteban (IDIBAPS, CIBERDEM) and Nawelle Dogheche (IDIBAPS) for their help in specific experiments, to Anna Soler (Hospital Clinic) for karyotyping the reprogrammed cells, and to Chris Newgard and Hans Hohmeier (Duke University) for critical reading of the manuscript. We thank the Advanced Optical Microscopy and the Electronic Microscopy Units of the Technological Centers of the University of Barcelona (CCiTUB for their help in sample processing and analyses. The monoclonal antibodies against C-peptide and Nkx2-2 were obtained from the Developmental Studies Hybridoma Bank developed under the auspices of the NICHD and maintained by The University of Iowa. This work has been supported by grant PI19/00896 (to RGa, RGo) integrated in the Plan Estatal de I+D+I and cofinanced by ISCIII-Subdirección General de Evaluación and Fondo Europeo de Desarrollo Regional (FEDER-"A way to build Europe"), grants 120230 (to RGa) and 121430/31/32 (to NM) from La Fundació La Marató de TV3, grant EFSF/JDRF/Lilly Type 1 Programme 2017 (to RGa) from the European Foundation for the Study of Diabetes, grants 2017 SGR 1166 (to JV) and 2017 SGR 1306 (to NM) from the Generalitat de Catalunya, by the Fundación DiabetesCERO and by the Cátedra Astra Zeneca. The research leading to these results has received funding from the European Community's Seventh Framework Programme (FP7/2009-2013) under the grant agreement nº229673 (SC) and from the European Research Council under the European Union's Horizon 2020 research and innovation programme-StG-2014-640525_REGMAMKID (NM). CIBERDEM (Centro de Investigación Biomédica en Red de Diabetes y Enfermedades Metabólicas Asociadas) is an initiative of the Instituto de Salud Carlos III.

AUTHOR CONTRIBUTIONS

Conceived and designed the experiments: MF, RGa. Performed the experiments: MF, AG, EP, NT, HF, RFR, SC. Provided human islets: CB, AW. Provided materials: LC,

JR, NM, AN. Analyzed and discussed the data: MF, CE, JV, RGo, RGa. Wrote the manuscript: MF, RGa.

CONFLICT OF INTEREST

Authors declare no conflict of interest

REFERENCES

1. Takahashi K, Tanabe K, Ohnuki M, Narita M, Ichisaka T, Tomoda K*, et al.* Induction of pluripotent stem cells from adult human fibroblasts by defined factors. *Cell* 2007, **131**(5)**:** 861-872.

2. Takahashi K, Yamanaka S. Induction of pluripotent stem cells from mouse embryonic and adult fibroblast cultures by defined factors. *Cell* 2006, **126**(4)**:** 663-676.

3. Graf T. Historical origins of transdifferentiation and reprogramming. *Cell stem cell* 2011, **9**(6)**:** 504-516.

4. Vierbuchen T, Wernig M. Molecular roadblocks for cellular reprogramming. *Molecular cell* 2012, **47**(6)**:** 827-838.

5. Xu J, Du Y, Deng H. Direct lineage reprogramming: strategies, mechanisms, and applications. *Cell stem cell* 2015, **16**(2)**:** 119-134.

6. Yamanaka S. A fresh look at iPS cells. *Cell* 2009, **137**(1)**:** 13-17.

7. D'Amour KA, Agulnick AD, Eliazer S, Kelly OG, Kroon E, Baetge EE. Efficient differentiation of human embryonic stem cells to definitive endoderm. *Nature biotechnology* 2005, **23**(12)**:** 1534-1541.

8. Kroon E, Martinson LA, Kadoya K, Bang AG, Kelly OG, Eliazer S*, et al.* Pancreatic endoderm derived from human embryonic stem cells generates glucose-responsive insulin-secreting cells in vivo. *Nature biotechnology* 2008, **26**(4)**:** 443-452.

9. Maehr R, Chen S, Snitow M, Ludwig T, Yagasaki L, Goland R*, et al.* Generation of pluripotent stem cells from patients with type 1 diabetes. *Proceedings of the National Academy of Sciences of the United States of America* 2009, **106**(37)**:** 15768-15773.

10. Pagliuca FW, Millman JR, Gurtler M, Segel M, Van Dervort A, Ryu JH*, et al.* Generation of functional human pancreatic beta cells in vitro. *Cell* 2014, **159**(2)**:** 428-439.

11. Rezania A, Bruin JE, Arora P, Rubin A, Batushansky I, Asadi A*, et al.* Reversal of diabetes with insulin-producing cells derived in vitro from human pluripotent stem cells. *Nature biotechnology* 2014, **32**(11)**:** 1121-1133.

12. Johnson JD. The quest to make fully functional human pancreatic beta cells from embryonic stem cells: climbing a mountain in the clouds. *Diabetologia* 2016, **59**(10)**:** 2047-2057.

13. Kushner JA, MacDonald PE, Atkinson MA. Stem cells to insulin secreting cells: two steps forward and now a time to pause? *Cell stem cell* 2014, **15**(5)**:** 535-536.

14. Zhou Q, Brown J, Kanarek A, Rajagopal J, Melton DA. In vivo reprogramming of adult pancreatic exocrine cells to beta-cells. *Nature* 2008, **455**(7213)**:** 627-632.

15. Ariyachet C, Tovaglieri A, Xiang G, Lu J, Shah MS, Richmond CA*, et al.* Reprogrammed Stomach Tissue as a Renewable Source of Functional beta Cells for Blood Glucose Regulation. *Cell stem cell* 2016, **18**(3)**:** 410-421.

16. Chen YJ, Finkbeiner SR, Weinblatt D, Emmett MJ, Tameire F, Yousefi M*, et al.* De novo formation of insulin-producing "neo-beta cell islets" from intestinal crypts. *Cell reports* 2014, **6**(6)**:** 1046-1058.

17. Furuyama K, Chera S, van Gurp L, Oropeza D, Ghila L, Damond N*, et al.* Diabetes relief in mice by glucose-sensing insulin-secreting human alpha-cells. *Nature* 2019.

18. Gasa R, Mrejen C, Leachman N, Otten M, Barnes M, Wang J*, et al.* Proendocrine genes coordinate the pancreatic islet differentiation program in vitro. *Proceedings of the National Academy of Sciences of the United States of America* 2004, **101**(36)**:** 13245-13250.

19. Heremans Y, Van De Casteele M, in't Veld P, Gradwohl G, Serup P, Madsen O*, et al.* Recapitulation of embryonic neuroendocrine differentiation in adult human pancreatic duct cells expressing neurogenin 3. *The Journal of cell biology* 2002, **159**(2)**:** 303-312.

20. Lee J, Sugiyama T, Liu Y, Wang J, Gu X, Lei J*, et al.* Expansion and conversion of human pancreatic ductal cells into insulin-secreting endocrine cells. *eLife* 2013, **2:** e00940.

21. Yechoor V, Liu V, Espiritu C, Paul A, Oka K, Kojima H*, et al.* Neurogenin3 is sufficient for transdetermination of hepatic progenitor cells into neo-islets in vivo but not transdifferentiation of hepatocytes. *Developmental cell* 2009, **16**(3)**:** 358-373.

22. Ieda M, Fu JD, Delgado-Olguin P, Vedantham V, Hayashi Y, Bruneau BG*, et al.* Direct reprogramming of fibroblasts into functional cardiomyocytes by defined factors. *Cell* 2010, **142**(3)**:** 375-386.

23. Hiramatsu K, Sasagawa S, Outani H, Nakagawa K, Yoshikawa H, Tsumaki N. Generation of hyaline cartilaginous tissue from mouse adult dermal fibroblast culture by defined factors. *The Journal of clinical investigation* 2011, **121**(2)**:** 640-657.

24. Vierbuchen T, Ostermeier A, Pang ZP, Kokubu Y, Sudhof TC, Wernig M. Direct conversion of fibroblasts to functional neurons by defined factors. *Nature* 2010, **463**(7284)**:** 1035-1041.

25. Najm FJ, Lager AM, Zaremba A, Wyatt K, Caprariello AV, Factor DC*, et al.* Transcription factor-mediated reprogramming of fibroblasts to expandable, myelinogenic oligodendrocyte progenitor cells. *Nature biotechnology* 2013, **31**(5)**:** 426-433.

26. Zhu S, Russ HA, Wang X, Zhang M, Ma T, Xu T*, et al.* Human pancreatic beta-like cells converted from fibroblasts. *Nature communications* 2016, **7:** 10080.

27. Pennarossa G, Maffei S, Campagnol M, Tarantini L, Gandolfi F, Brevini TA. Brief demethylation step allows the conversion of adult human skin fibroblasts into insulin-secreting cells. *Proceedings of the National Academy of Sciences of the United States of America* 2013, **110**(22)**:** 8948-8953.

28. Pereyra-Bonnet F, Gimeno ML, Argumedo NR, Ielpi M, Cardozo JA, Gimenez CA*, et al.* Skin fibroblasts from patients with type 1 diabetes (T1D) can be chemically transdifferentiated into insulin-expressing clusters: a transgene-free approach. *PloS one* 2014, **9**(6)**:** e100369.

29. Akinci E, Banga A, Tungatt K, Segal J, Eberhard D, Dutton JR*, et al.* Reprogramming of various cell types to a beta-like state by Pdx1, Ngn3 and MafA. *PloS one* 2013, **8**(11)**:** e82424.

30. Katz LS, Geras-Raaka E, Gershengorn MC. Reprogramming adult human dermal fibroblasts to islet-like cells by epigenetic modification coupled to transcription factor modulation. *Stem cells and development* 2013, **22**(18)**:** 2551-2560.

31. Broca C, Varin E, Armanet M, Tourrel-Cuzin C, Bosco D, Dalle S*, et al.* Proteasome dysfunction mediates high glucose-induced apoptosis in rodent beta cells and human islets. *PloS one* 2014, **9**(3)**:** e92066.

32. Lynn FC, Sanchez L, Gomis R, German MS, Gasa R. Identification of the bHLH factor Math6 as a novel component of the embryonic pancreas transcriptional network. *PloS one* 2008, **3**(6)**:** e2430.

33. Bartholomeus K, Jacobs-Tulleneers-Thevissen D, Shouyue S, Suenens K, In't Veld PA, Pipeleers-Marichal M*, et al.* Omentum is better site than kidney capsule for growth, differentiation, and vascularization of immature porcine beta-cell implants in immunodeficient rats. *Transplantation* 2013, **96**(12)**:** 1026-1033.

34. Figueiredo H, Figueroa ALC, Garcia A, Fernandez-Ruiz R, Broca C, Wojtusciszyn A*, et al.* Targeting pancreatic islet PTP1B improves islet graft revascularization and transplant outcomes. *Science translational medicine* 2019, **11**(497).

35. Li W, Nakanishi M, Zumsteg A, Shear M, Wright C, Melton DA*, et al.* In vivo reprogramming of pancreatic acinar cells to three islet endocrine subtypes. *eLife* 2014, **3:** e01846.

36. Granio O, Porcherot M, Corjon S, Kitidee K, Henning P, Eljaafari A*, et al.* Improved adenovirus type 5 vector-mediated transduction of resistant cells by piggybacking on coxsackie B-adenovirus receptor-pseudotyped baculovirus. *Journal of virology* 2009, **83**(12)**:** 6048-6066.

37. Toh ML, Hong SS, van de Loo F, Franqueville L, Lindholm L, van den Berg W, *et al.* Enhancement of adenovirus-mediated gene delivery to rheumatoid arthritis synoviocytes and synovium by fiber modifications: role of arginine-glycine-aspartic acid (RGD)- and non-RGD-binding integrins. *Journal of immunology* 2005, **175**(11)**:** 7687-7698.

38. Fontcuberta-PiSunyer M, Cervantes S, Miquel E, Mora-Castilla S, Laurent LC, Raya A*, et al.* Modulation of the endocrine transcriptional program by targeting histone modifiers of the H3K27me3 mark. *Biochimica et biophysica acta* 2018, **1861**(5)**:** 473-480.

39. Tomaru Y, Hasegawa R, Suzuki T, Sato T, Kubosaki A, Suzuki M*, et al.* A transient disruption of fibroblastic transcriptional regulatory network facilitates trans-differentiation. *Nucleic acids research* 2014, **42**(14)**:** 8905-8913.

40. Ramzy AK, T.J. Revisiting Proinsulin Processing: Evidence That Human β-Cells Process Proinsulin With Prohormone Convertase (PC) 1/3 but Not PC2. *Diabetes* 2020, **69:** 1451-1462.

41. Schuit FVL, J; Granvik,M; Goyvaerts, L; de Faudeur, Gd, Schraenen, A; Lemaire, K. b-Cell–Specific Gene Repression: A Mechanism to Protect Against Inappropriate or Maladjusted Insulin Secretion? *Diabetes* 2012, **61:** 969-975.

42. Brereton MF, Vergari E, Zhang Q, Clark A. Alpha-, Delta- and PP-cells: Are They the Architectural Cornerstones of Islet Structure and Co-ordination? . *J Histochem Cytochem* 2015, **63:** 575-591.

43. D'Amour KA, Bang AG, Eliazer S, Kelly OG, Agulnick AD, Smart NG*, et al.* Production of pancreatic hormone-expressing endocrine cells from human embryonic stem cells. *Nature biotechnology* 2006, **24**(11)**:** 1392-1401.

44. Adeghate E, Donath T. Morphological findings in long-term pancreatic tissue transplants in the anterior eye chamber of rats. *Pancreas* 1990, **5**(3)**:** 298-305.

45. Leibiger IB, Berggren PO. Intraocular in vivo imaging of pancreatic islet cell physiology/pathology. *Molecular metabolism* 2017, **6**(9)**:** 1002-1009.

46. Sapir T, Shternhall K, Meivar-Levy I, Blumenfeld T, Cohen H, Skutelsky E*, et al.* Cell-replacement therapy for diabetes: Generating functional insulin-producing tissue from adult human liver cells. *Proceedings of the National Academy of Sciences of the United States of America* 2005, **102**(22)**:** 7964-7969.

47. Russ HA, Parent AV, Ringler JJ, Hennings TG, Nair GG, Shveygert M*, et al.* Controlled induction of human pancreatic progenitors produces functional beta-like cells in vitro. *The EMBO journal* 2015, **34**(13)**:** 1759-1772.

48. Rezania A, Bruin JE, Xu J, Narayan K, Fox JK, O'Neil JJ*, et al.* Enrichment of human embryonic stem cell-derived NKX6.1-expressing pancreatic progenitor cells accelerates the maturation of insulin-secreting cells in vivo. *Stem cells* 2013, **31**(11)**:** 2432-2442.

49. Rezania A, Bruin JE, Riedel MJ, Mojibian M, Asadi A, Xu J*, et al.* Maturation of human embryonic stem cell-derived pancreatic progenitors into functional islets

capable of treating pre-existing diabetes in mice. *Diabetes* 2012, **61**(8)**:** 2016-2029.

50. Liu H, Li R, Liao H-K, Min Z, Wang C, Yu Y*, et al.* Chemical combinations potentiate human pluripotent stem cell-derived 3D pancreatic progenitor clusters toward functional β cell. *Nature communications* 2021, **12:** 3330.

51. Hrvatin S, O'Donnell CW, Deng F, Millman JR, Pagliuca FW, DiIorio P*, et al.* Differentiated human stem cells resemble fetal, not adult, beta cells. *Proceedings of the National Academy of Sciences of the United States of America* 2014, **111**(8)**:** 3038-3043.

52. Bruin JE, Rezania A, Xu J, Narayan K, Fox JK, O'Neil JJ*, et al.* Maturation and function of human embryonic stem cell-derived pancreatic progenitors in macroencapsulation devices following transplant into mice. *Diabetologia* 2013, **56**(9)**:** 1987-1998.

53. Liu ML, Zang T, Zou Y, Chang JC, Gibson JR, Huber KM*, et al.* Small molecules enable neurogenin 2 to efficiently convert human fibroblasts into cholinergic neurons. *Nature communications* 2013, **4:** 2183.

54. Zhu S, Li W, Zhou H, Wei W, Ambasudhan R, Lin T*, et al.* Reprogramming of human primary somatic cells by OCT4 and chemical compounds. *Cell stem cell* 2010, **7**(6)**:** 651-655.

55. Ma X, Zhu S. **Chemical strategies for pancreatic β cell differentiation, reprogramming, and regeneration**. *Acta Biochim Biophys Sin (Shanghai)* 2017, **49:** 289-301.

56. Hu W, Qiu B, Guan W, Wang Q, Wang M, Li W*, et al.* Direct Conversion of Normal and Alzheimer's Disease Human Fibroblasts into Neuronal Cells by Small Molecules. *Cell stem cell* 2015, **17**(2)**:** 204-212.

57. Li K, Zhu S, Russ HA, Xu S, Xu T, Zhang Y*, et al.* Small molecules facilitate the reprogramming of mouse fibroblasts into pancreatic lineages. *Cell stem cell* 2014, **14**(2)**:** 228-236.

58. Fu Y, Huang C, Xu X, Gu H, Ye Y, Jiang C*, et al.* Direct reprogramming of mouse fibroblasts into cardiomyocytes with chemical cocktails. *Cell research* 2015, **25**(9)**:** 1013-1024.

FIGURE LEGENDS

Figure 1. Introduction of the PNM factors in human fibroblasts.

Human foreskin fibroblasts (HFF1) were transduced with a polycistronic recombinant adenovirus encoding the transcription factors Pdx1, Neurog3, MafA and the reporter

protein Cherry (Ad-PNM). Untreated parental fibroblasts were used as controls (indicated as C in graphs). **(A)** Bright field images and Cherry immunofluorescence of control fibroblasts and fibroblasts infected with Ad-PNM at day 3 and 7 post-infection. Scale bar is 100 µm. **(B)** qRT-PCR of adenovirus-encoded transgenes at day 3 (n=11) and 7 (n=6) after infection with Ad-PNM**. (C)** qRT-PCR of human *INS* at day 3 (n=7) and 7 (n=13) after infection with Ad-PNM. (**D)** In red, qRT-PCR of human *INS* in fibroblasts maintained in the indicated culture media during 7 days after infection with the indicated adenoviruses, (n=3-10). In blue, *INS* mRNA levels in iPSC-derived β-cells and in isolated human islets (n=10). **(E-F)** qRT-PCR of indicated genes encoding islet/β-cell transcription factors and islet hormones at day 7 post-PNM (n=8-15). **(G)** qRT-PCR for the indicated fibroblast markers at days 3 (n=5-11) and 7 post-PNM (n=5-6). In **B-F**, expression levels are expressed relative to *TBP.* In ***G***, expression is relative to control fibroblasts, given the value of 1 (dotted line). Data are presented as the mean ± SEM for the number of samples indicated in parenthesis. *,P<0.05; **,P<0.01; ***,P<0.001, relative to control (untreated) fibroblasts or between indicated conditions using unpaired t-test (**B-E**) or one sample t-test (**G**).

Figure 2. Sequential introduction of the PNM factors, Pax4 and Nkx2-2 (5 TF protocol) in human fibroblasts.

(A) qRT-PCR for the indicated genes in HFF1 fibroblasts infected with different combinations of the indicated adenoviruses. Pax4 was added three days after PNM. Nkx2-2 was added three days (PNM+Nkx2-2) or six days (PNM+Pax4+Nkx2-2) after PNM. Expression levels are calculated relative to *TBP* (n=4-12). **(B)** Scheme of the final 5TF reprogramming protocol showing the sequence of addition of adenoviruses encoding the indicated transcription factor/s. Duration of incubation with each adenovirus is represented with a line. Cells were studied at days 9-10 after initial addition of Ad-PNM. **(C)** Representative bright field image of parental fibroblasts and 5TF reprogrammed fibroblasts at day 10. **(D)** Cell proliferation measured by BrdU

incorporation (n=3) and **(E)** Cell viability measured by MTT assay (n=3) in untreated control (in black) and 5TF-reprogrammed fibroblasts (in red) at the indicated days. Day 4 values are before Pax4 introduction. **(F-G)** Representative immunofluorescence images showing Insulin and C-peptide staining (in red) in untreated fibroblasts and in fibroblasts infected with Ad-PNM alone or with 5TF. Nuclei were stained with Hoechst (in blue). Scale bar is 25 µm. Data are presented as the mean ± SEM for the number of experiments indicated in parenthesis *,P<0.05; **,P<0.01; ***,P<0.001, P<0.0001 relative to PNM (in **A**) or to control fibroblasts (**D,E**) using one-way ANOVA (**A**), one-sample t-test (**D**) or unpaired t-test (**E**).

Figure 3. 5FT protocol promotes β-cell specific gene activation and repression events in human fibroblasts.

(A,B) qRT-PCR of islet/β-cell transcription factor **(A)** and β-cell function **(B)** genes in untreated control fibroblasts (n=5-19), in fibroblasts infected with Ad-PNM alone (n=3-20) or with 5TF (n=5-18) and in human islets (n=6-9). **(C)** qRT-PCR of β-cell disallowed genes in untreated control fibroblasts (n=5), in fibroblasts infected with 5TF (n=5-8) and in human islets (n=5). Expression levels were calculated relative to *TBP*. Values represent the mean ± SEM for 5-14 for the number of n indicated in parenthesis *, P< 0.05, **, P< 0.01, ***, P< 0.001 between indicated bars using unpaired t-test.

Figure 4. Functional characterization of iβ-like cells generated with the 5TF protocol.

iβ-like cells were loaded with the calcium indicator Fluo-4-AM at day 10 of the 5TF protocol. Single-cell imaging to detect cytosolic calcium was performed in the following sequence: low glucose (2mM, G2), high glucose (20mM, G20) and membrane depolarization with KCl 30mM. **(A)** Quantification of the frequency of cells (n=200, from 6 independent reprogramming experiments) that responded to glucose, membrane

depolarization elicited by high potassium or both. Representative measurements of dynamic Fluo-4 fluorescence for **(B)** six single fibroblasts and **(C)** four single iβ-like cells. **(D)** In vitro insulin secretion by iβ-like cells. ELISA determination of secreted human insulin by control fibroblasts and iβ-like cells under non-stimulatory conditions (glucose 2mM) and stimulatory conditions (glucose 20 mM). Data are mean ± SEM for 6 independent reprogramming experiments.

Figure 5. In vitro characterization of iβ-like cell spheroids.

(A) Schematic representation of the modified 5TF protocol: cells were moved from 2D to 3D culture during the last three days (days 7-10) of the protocol. Bright field image of generated iβ-like cell spheroids. Scale bar is 100 μm. **(B)** Representative immunofluorescence image showing C-peptide staining in red and nuclei in blue (marked with Hoechst) of an iβ-like cell spheroid at the end of the reprogramming protocol. Scale bar is 100 μm. **(C)** qRT-PCR of the indicated genes in iβ-like cell spheroids (n=9-16). Transcript levels are expressed as fold relative to levels in iβ-like cells maintained in 2D culture throughout the 10-day protocol (given the value of 1, dotted line). **(D)** In vitro glucose-induced insulin secretion by iβ-like cell spheroids (n=14, from 8 reprogramming experiments). Secretion by control spheroids composed of parental fibroblasts (n= 5) is also shown. **(E)** Glucose secretory Index (fold-response 20mM vs. 2mM glucose) of iβ-like cells maintained in 2D or in 3D (spheroids) cultures (n=16-18, from 8-10 reprogramming experiments). **(F)** Glucose dose curve of insulin secretion by iβ-like cell spheroids (n=4-12, 5 reprogramming experiments). **(G)** Conventional transmission electron microscopy showing a representative image of iβ-like cell spheroids. Prototypical electron dense secretory vesicles (asterisks) are observed dispersed in the cytoplasm. Well-preserved mitochondria (mit), endoplasmic reticulum (ER), Golgi membranes (G) and lipid droplets (LD) are also observed. Inset shows a detail of a secretory vesicle with an average diameter of 450nm. N, nucleus.

Scale bars are 200nm (inset) and 500nm. Data are presented as the mean ± SEM for the number of experiments (n) indicated in parenthesis. *,P<0.05; **,P<0.01; ***,P<0.001, relative to 2D iβ cells **(C,E)**, or between glucose concentrations **(D,F)** using one sample t-test (**C**), unpaired t test **(D, E)** or one-way ANOVA **(F).**

Figure 6. In vivo characterization of iβ-like cell spheroids.

(A) Schematic representation of the transplantation of iβ-like cell spheroids into the anterior chamber of the eye (ACE) of immunodeficient NSG mice. **(B)** Image of an eye recently transplanted with 300 iβ-like cell spheroids (1000 cells/spheroid). **(C)** Vascularization of iβ-like cell aggregate grafts ten days following transplantation into the ACE. Representative in vivo image of functional vessels (RITC-dextran, red) and viable iβ-like cells (CFDA, green). Scale bar is 100 µm. **(D)** qRT-PCR of human *TBP* and human INS transcripts in eyes of non-transplanted mice (n=3) and mice transplanted with fibroblast spheroids (n=3) or iβ-like cell spheroids (n=5) collected ten days post-transplantation. Human *TBP* expression is calculated relative to mouse*Tbp* and human *INS* relative to human *TBP*. **(E)** Representative immunofluorescence images showing HLA staining in red and C-peptide staining in green in iβ-like cell spheroid grafts ten days post-transplantation in NSG mice. Scale bar is 25 µm. **(F)** Percentage of C-peptide+/HLA+ in eye grafts ten days after transplantation (n=5). **(G)** ELISA determination of human insulin in the aqueous humor after a glucose bolus in un-transplanted mice (n=7), in control mice transplanted with fibroblast spheroids (n=16) and in mice transplanted with iβ-like cell spheroids (n= 17) in the ACE at day 10 post-transplantation; and in mice transplanted with 150-200 human islets (n=3) in the ACE at day 12-15 post-transplantation. **(H)** ELISA determination of human insulin in plasma, before and after a glucose challenge, at days 15 and 30 after transplantation of iβ-like cell spheroids subcutaneously (n=3) or in the omentum (n=3) of NSG mice. Each individual mouse is represented by a different color. Plasma human insulin levels

in non-transplanted animals (n=3), before and after glucose administration, and in animals transplanted with human islets in the ACE (n=5), after a glucose bolus, are provided for comparison purposes. Data are presented as mean ± SEM. ***, P< 0.001 using unpaired t-test.

Figure 1

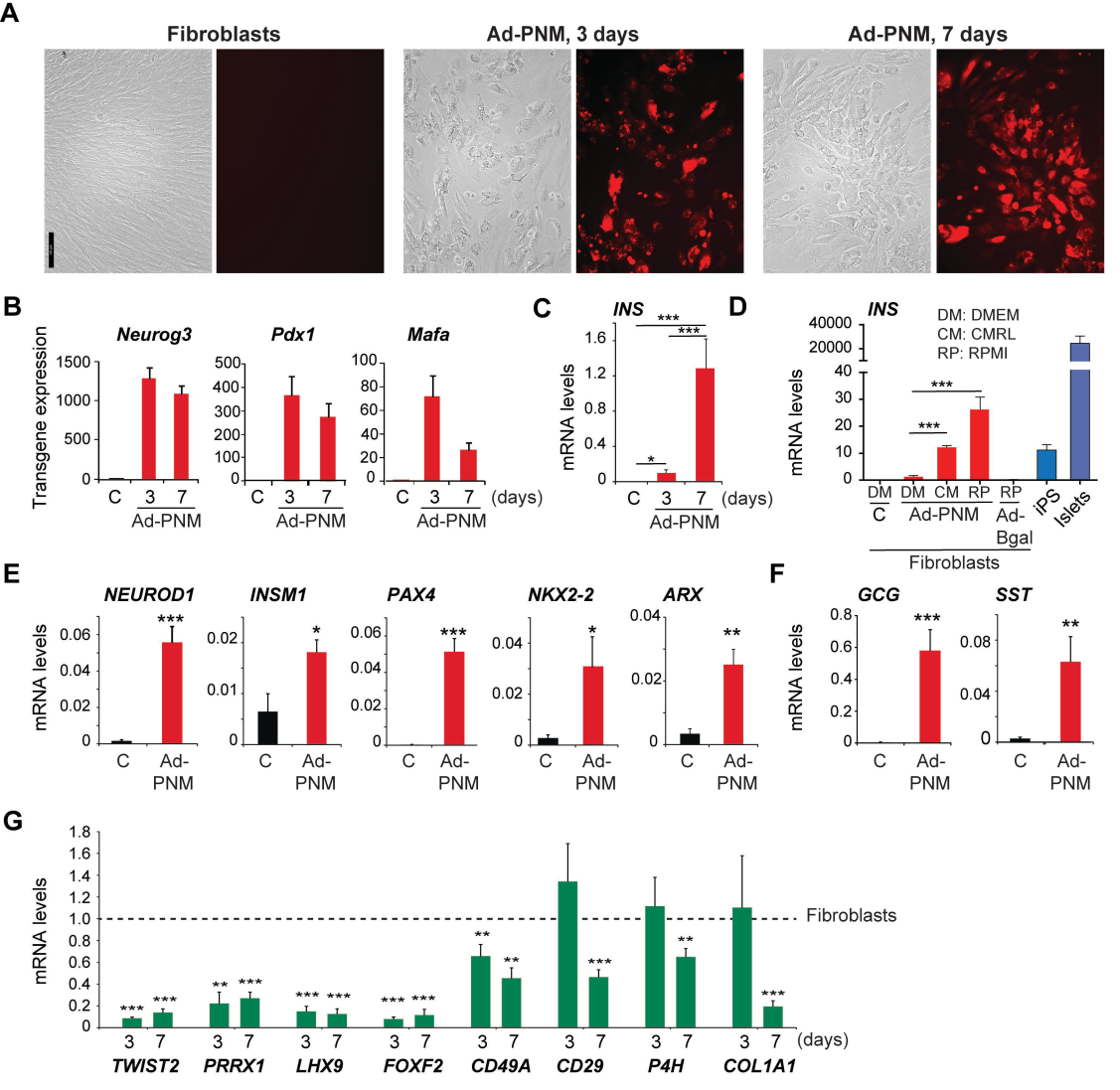
A
Fibroblasts
Ad-PNM, 3 days
Ad-PNM, 7 days
B
Neurog3
Pdx1
Mafa
Transgene expression
C 3 7 (days)
Ad-PNM
C
INS
mRNA levels
D
INS
DM: DMEM
CM: CMRL
RP: RPMI
DM C
DM CM RP Ad-PNM
RP Ad-Bgal
iPS
Islets
Fibroblasts
E
NEUROD1
INSM1
PAX4
NKX2-2
ARX
C Ad-PNM
F
GCG
SST
G
Fibroblasts
TWIST2
PRRX1
LHX9
FOXF2
CD49A
CD29
P4H
COL1A1

Figure 2

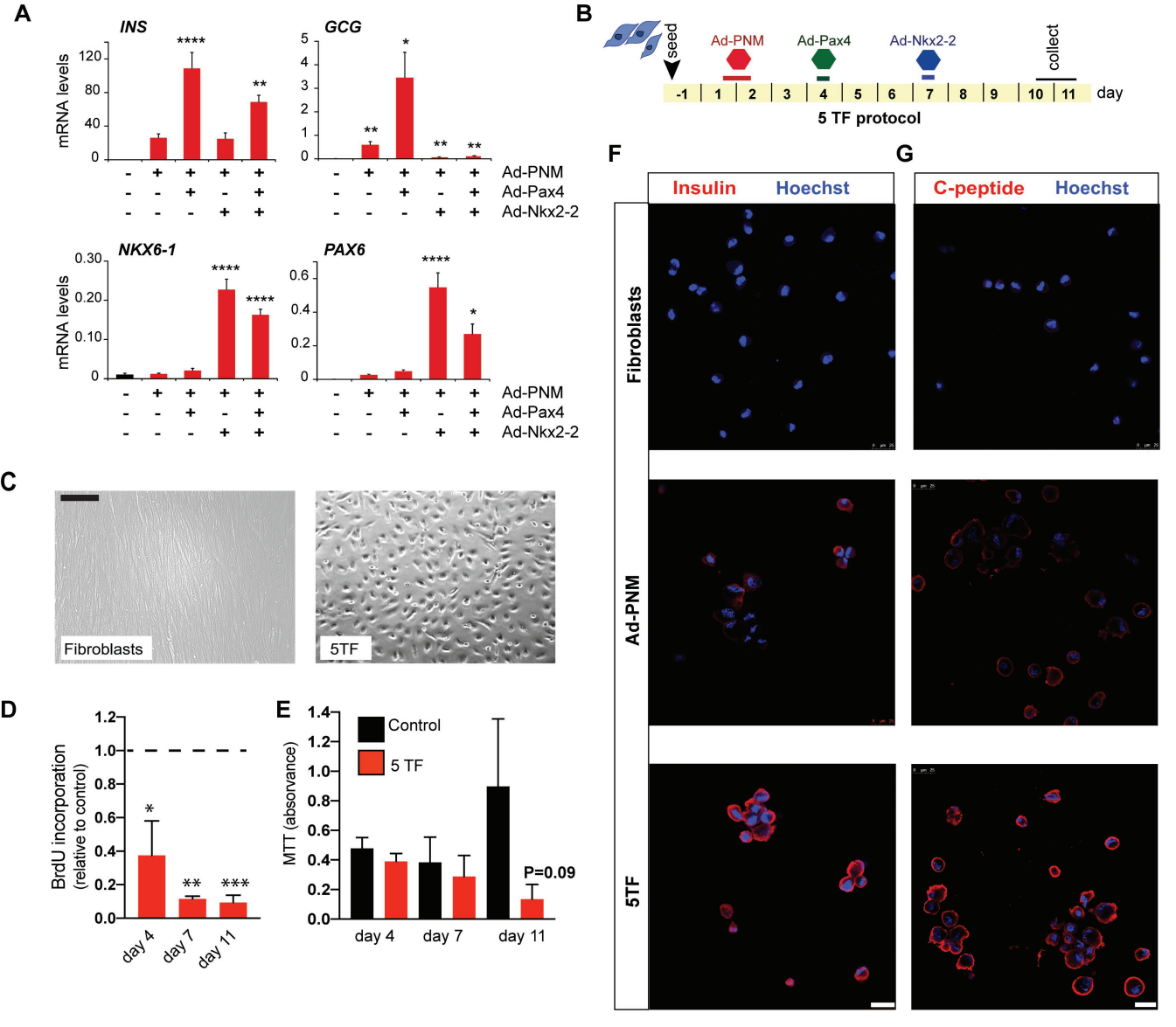
A
INS
GCG
NKX6-1
PAX6
mRNA levels
Ad-PNM
Ad-Pax4
Ad-Nkx2-2
B
seed
Ad-PNM
Ad-Pax4
Ad-Nkx2-2
collect
day
5 TF protocol
C
Fibroblasts
5TF
D
BrdU incorporation (relative to control)
day 4
day 7
day 11
E
MTT (absorvance)
Control
5 TF
P=0.09
F
G
Insulin
Hoechst
C-peptide
Hoechst
Fibroblasts
Ad-PNM
5TF

Figure 3

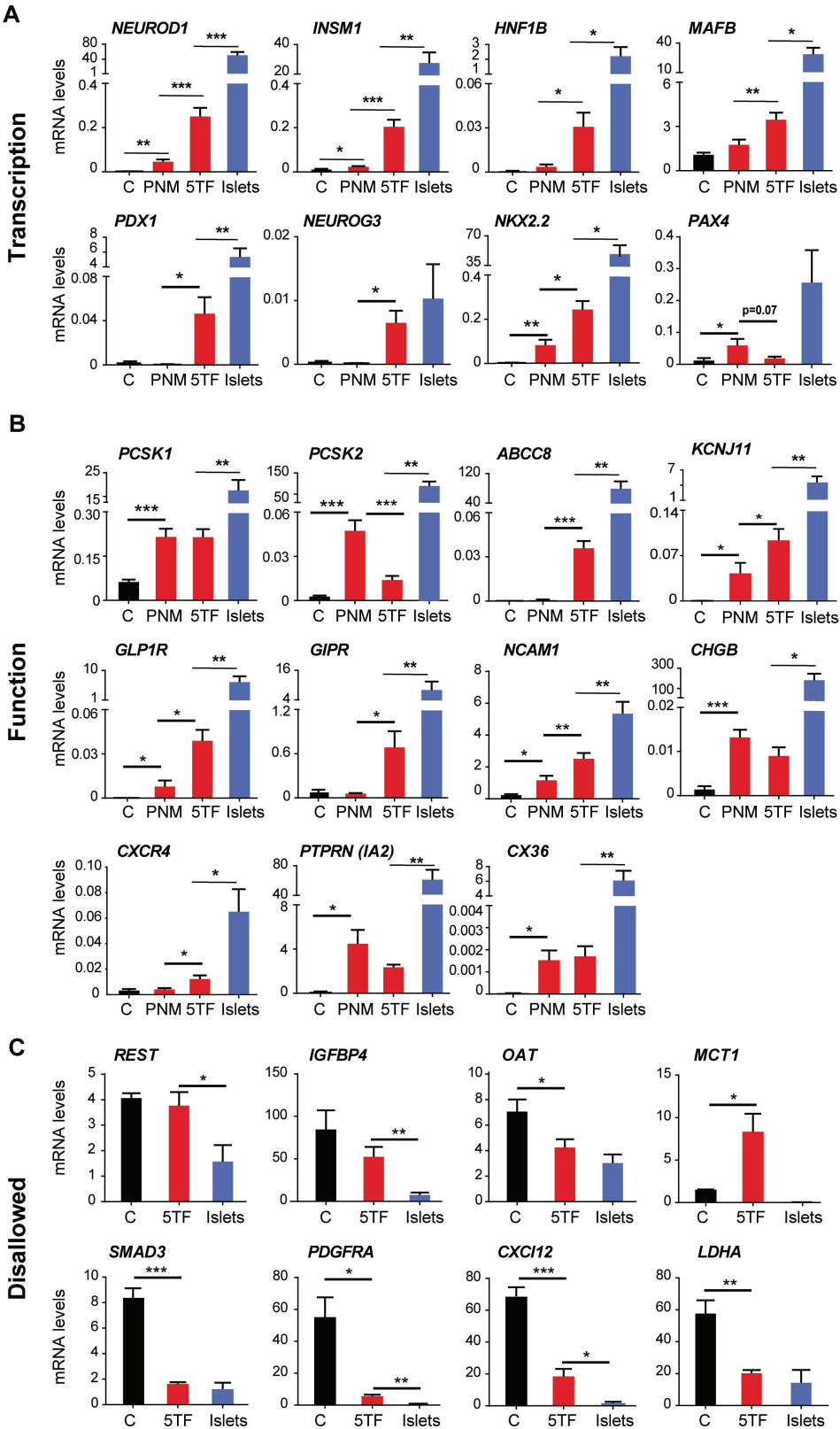
A
Transcription
NEUROD1
INSM1
HNF1B
MAFB
PDX1
NEUROG3
NKX2.2
PAX4
p=0.07
B
Function
PCSK1
PCSK2
ABCC8
KCNJ11
GLP1R
GIPR
NCAM1
CHGB
CXCR4
PTPRN (IA2)
CX36
C
Disallowed
REST
IGFBP4
OAT
MCT1
SMAD3
PDGFRA
CXCl12
LDHA
mRNA levels
C
PNM
5TF
Islets

Figure 4

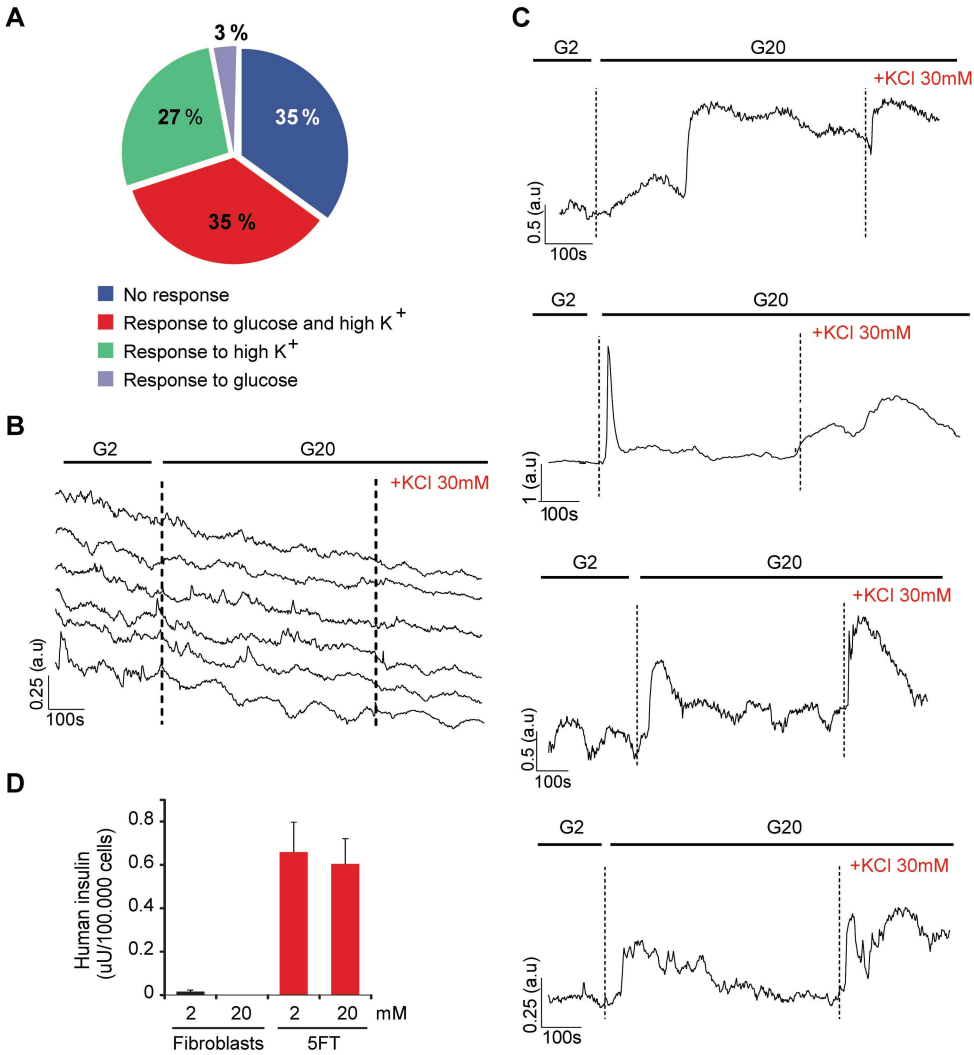
A
3 %
27 %
35 %
35 %
No response
Response to glucose and high K+
Response to high K+
Response to glucose
B
G2
G20
+KCl 30mM
0.25 (a.u)
100s
C
G2
G20
+KCl 30mM
0.5 (a.u)
100s
G2
G20
+KCl 30mM
1 (a.u)
100s
G2
G20
+KCl 30mM
0.5 (a.u)
100s
G2
G20
+KCl 30mM
0.25 (a.u)
100s
D
Human insulin (uU/100.000 cells)
0.8
0.6
0.4
0.2
0
2
20
2
20
mM
Fibroblasts
5FT

Figure 5

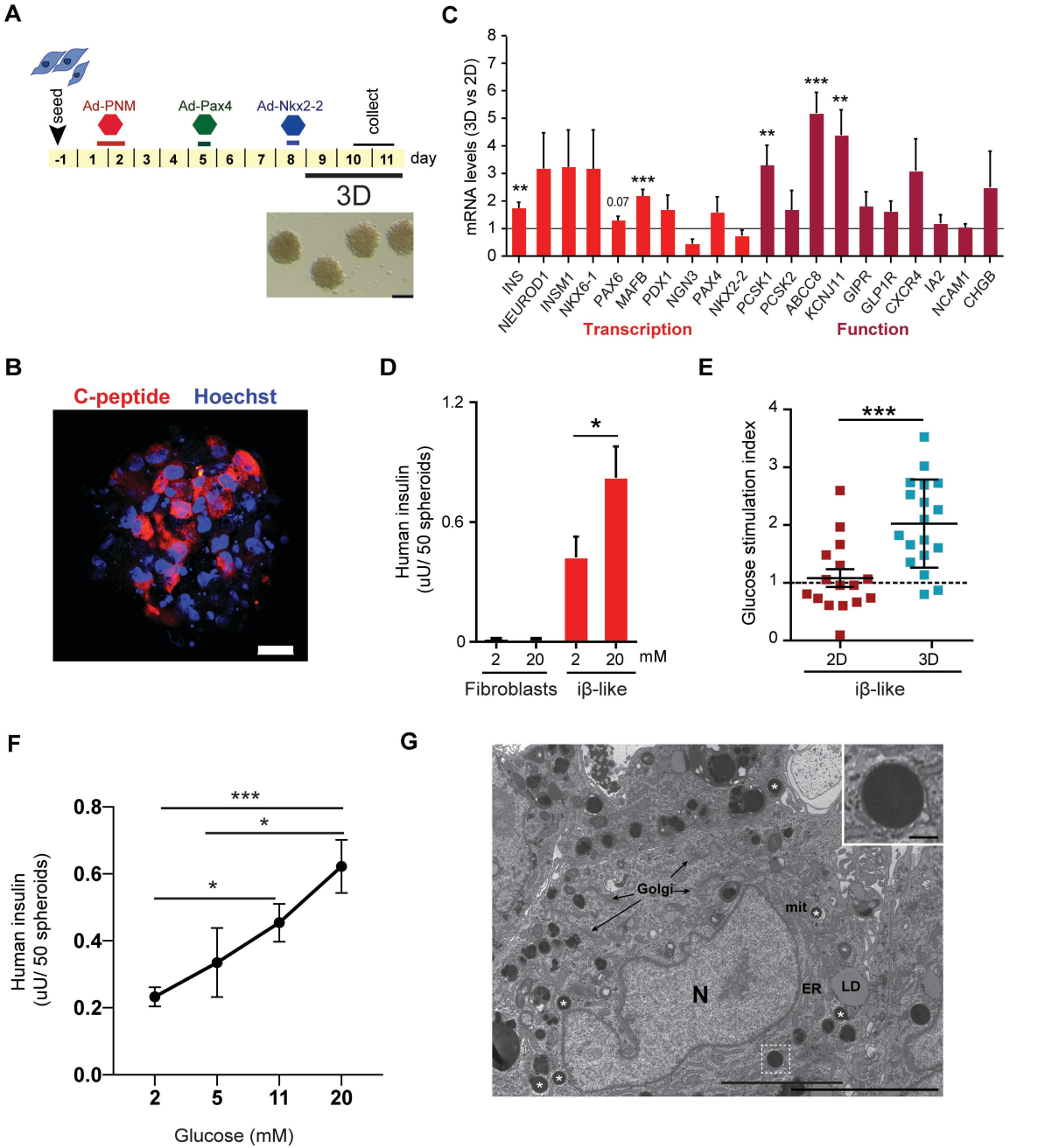
A
seed
Ad-PNM
Ad-Pax4
Ad-Nkx2-2
collect
-1 1 2 3 4 5 6 7 8 9 10 11 day
3D
B
C-peptide
Hoechst
C
mRNA levels (3D vs 2D)
INS
NEUROD1
INSM1
NKX6-1
PAX6
MAFB
PDX1
NGN3
PAX4
NKX2-2
PCSK1
PCSK2
ABCC8
KCNJ11
GIPR
GLP1R
CXCR4
IA2
NCAM1
CHGB
Transcription
Function
D
Human insulin (uU/ 50 spheroids)
2 20 2 20 mM
Fibroblasts
iβ-like
E
Glucose stimulation index
2D
3D
iβ-like
F
Human insulin (uU/ 50 spheroids)
Glucose (mM)
G
Golgi
mit
N
ER
LD

Figure 6

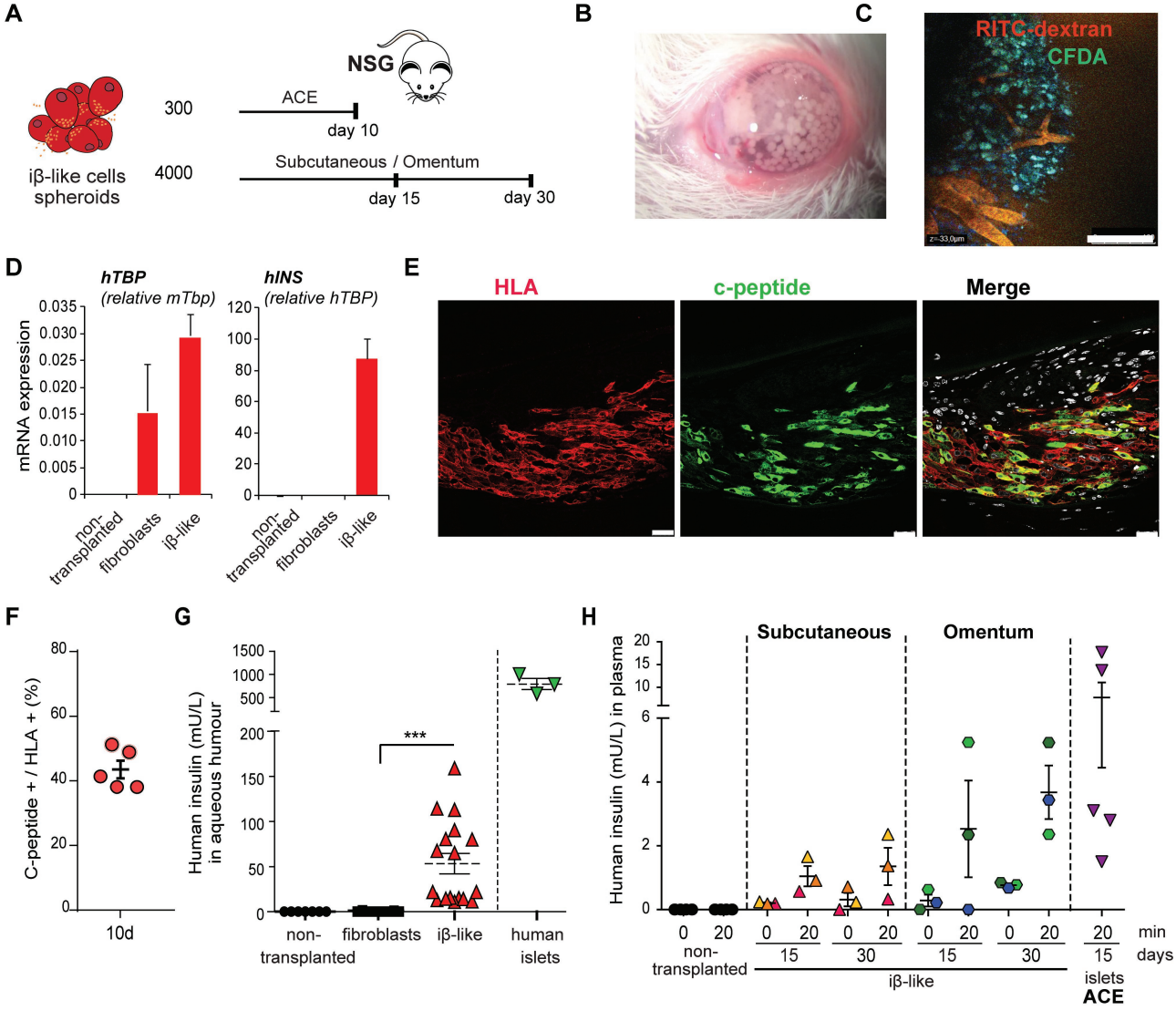
A
NSG
300
ACE
day 10
iβ-like cells spheroids
4000
Subcutaneous / Omentum
day 15
day 30
B
C
RITC-dextran
CFDA
D
hTBP
(relative mTbp)
hINS
(relative hTBP)
mRNA expression
non-transplanted
fibroblasts
iβ-like
E
HLA
c-peptide
Merge
F
C-peptide + / HLA + (%)
10d
G
Human insulin (mU/L) in aqueous humour
***
non-transplanted
fibroblasts
iβ-like
human islets
H
Human insulin (mU/L) in plasma
Subcutaneous
Omentum
min
days
non-transplanted
iβ-like
islets
ACE

Supplemental information

for

DIRECT REPROGRAMMING OF HUMAN FIBROBLASTS INTO INSULIN-PRODUCING CELLS BY TRANSCRIPTION FACTORS

Marta Fontcuberta-PiSunyer, Ainhoa García-Alamán, Èlia Prades, Noèlia Téllez, Hugo Figueiredo, Rebeca Fernandez-Ruiz, Sara Cervantes, Carlos Enrich, Laura Clua, Javier Ramón-Azcón, Christophe Broca, Anne Wojtusciszyn, Anna Novials, Nuria Montserrat, Josep Vidal, Ramon Gomis, Rosa Gasa

This document contains:

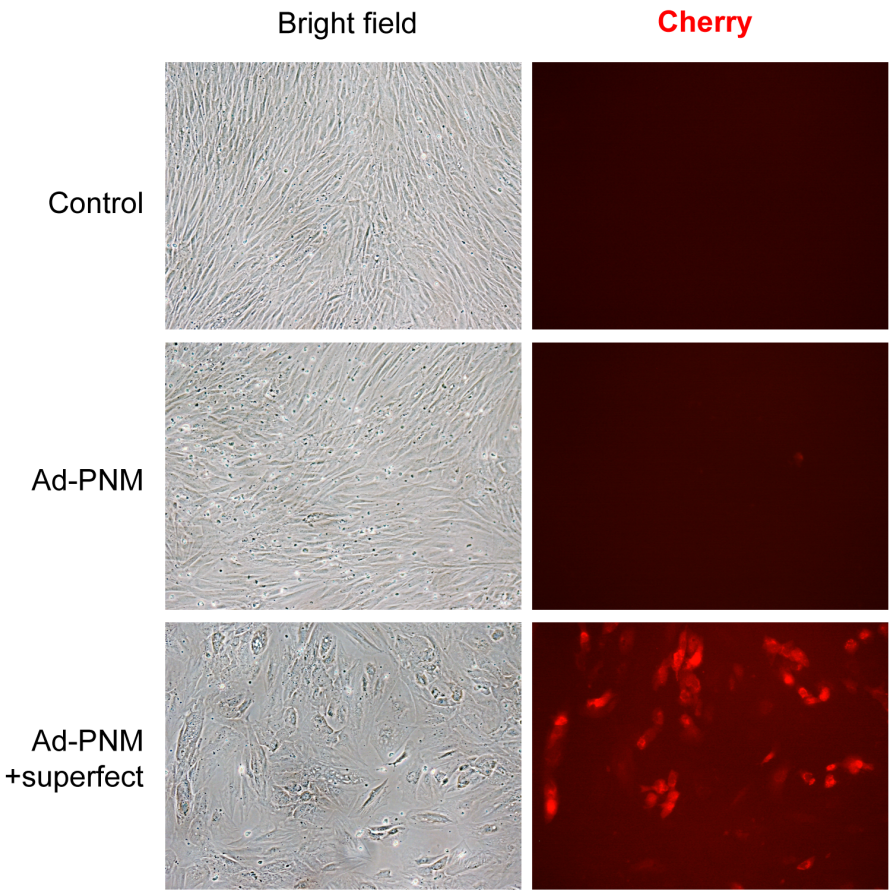

Supplementary S1. Human primary foreskin fibroblasts HFF1 were treated for 14h with a polycistronic recombinant adenovirus (Ad-PNM) encoding the PNM factors (Pdx1, Neurog3 and Mafa) and a Cherry reporter protein, in the presence or absence of the Superfect transfection reagent. Bright field and Cherry immunofluorescence images from control (parental) fibroblasts and HFF1 fibroblasts four days after infection.

A

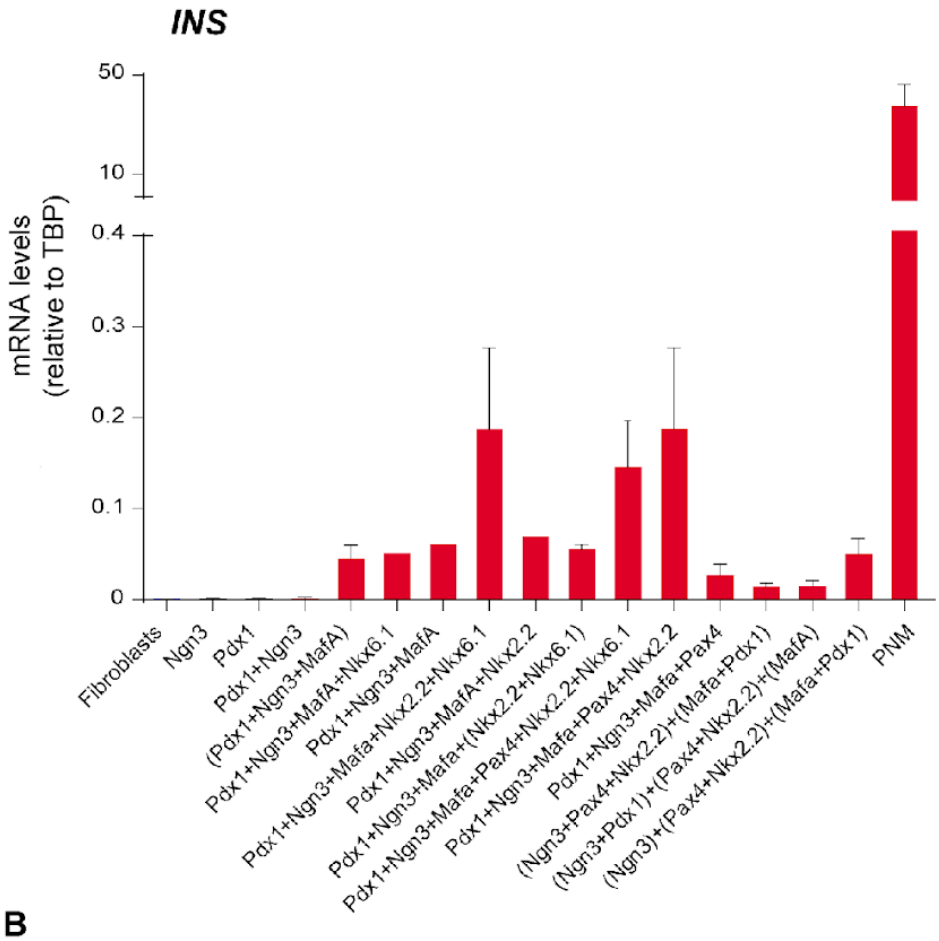

B

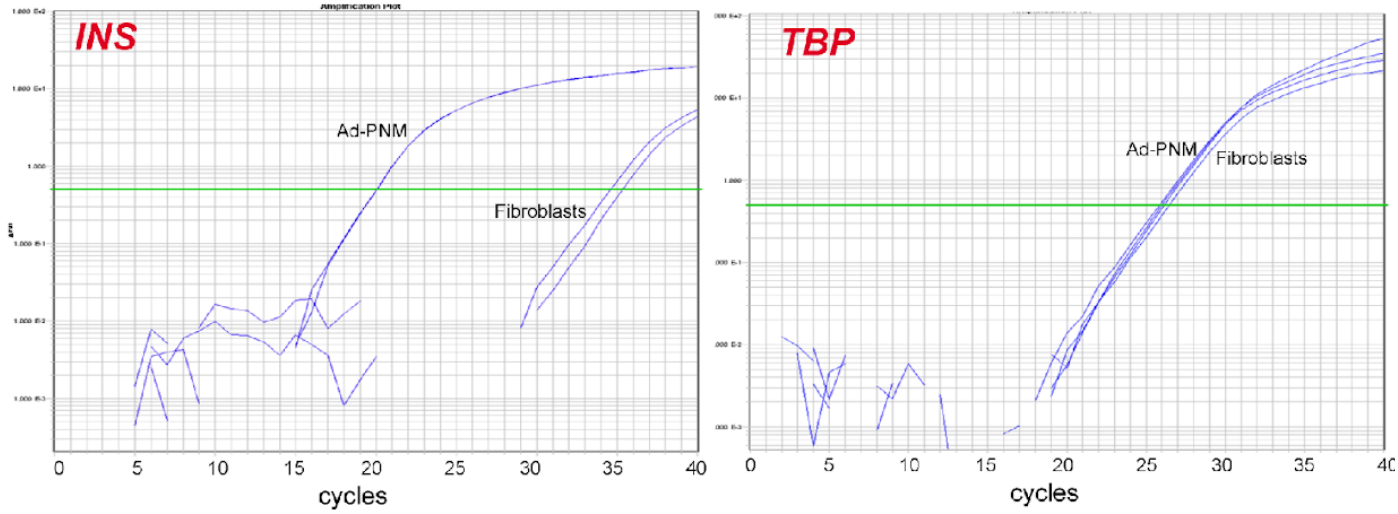

Supplementary S2. (A) qRT-PCR for human *INS* in human foreskin fibroblasts HFF1 ten days after infection with the recombinant adenoviruses encoding the indicated transcription factors. All adenoviruses except Ad-PNM encoded a single transcription factor. Adenoviruses that were added simultaneously are shown in parenthesis. Order of addition is left to right. Expression levels were calculated relative to *TBP*. Data are mean ± SEM for n=2-9. **(B)** Real time amplification plots for *INS* and *TBP* in parental fibroblasts and in fibroblasts seven days after infection with Ad-PNM.

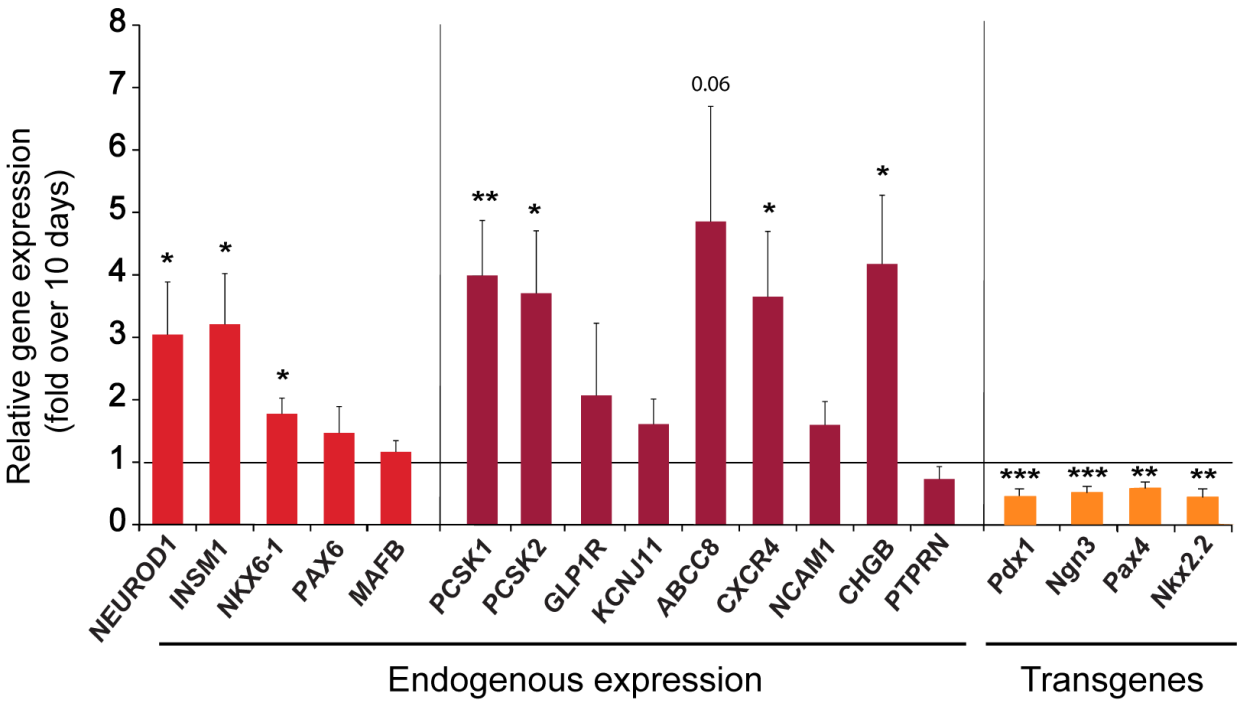

Supplementary S3: qRT-PCR of the indicated genes at day 21 after initiation of reprogramming. Transcript levels are expressed relative to levels in cells at day 10 of the reprogramming protocol (given the value of 1). Cells were maintained in 2D culture throughout the duration of the experiment. Data are mean ± SEM for n=9-13, from 7 reprogramming experiments. *P< 0.05, **P< 0.01, ***, P< 0.001, vs. iβ-cells at day10 using

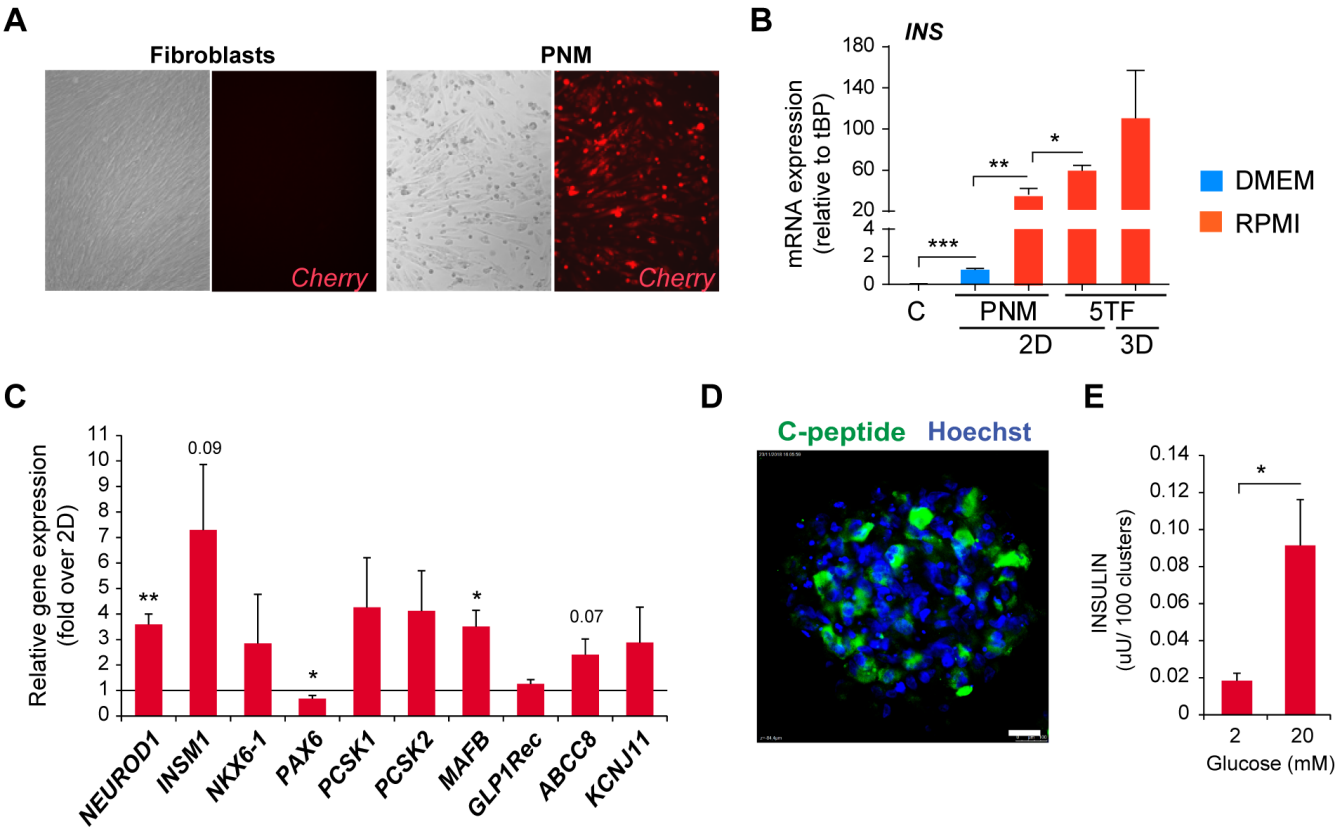

Supplementary S4: Human primary foreskin fibroblasts HFF2 were subjected to transcription factor-based reprogramming towards insulin-producing cells. **(A)** Bright field and Cherry immunofluorescence images from control (parental) fibroblasts and from fibroblasts three days after infection with Ad-PNM. Scale bar is 100 uM. **(B)** qRT-PCR for *INS* in HFF2 ten days after infection with Ad-PNM alone and cultured under 2D conditions in DMEM (blue) or RPMI-1640 media (red) (n=6), or subjected to the 5TF reprogramming protocol and cultured in RPMI-1640 media under 2D or 3D (n=4) conditions as indicated. Expression levels were calculated relative to *TBP*. Note that changes in *INS* gene expression in the different reprogramming conditions follow a similar trend as observed with HFF1 fibroblasts. **(C)** qRT-PCR of the indicated genes in HFF2-derived iβ-like cell spheroids (n=6) Transcript levels are expressed relative to HFF2-derived iβ-like cells maintained in 2D culture throughout the 10-day protocol (given the value of 1). **(D)** Representative immunofluorescence image showing C-peptide staining in green and nuclei in blue (marked with Hoechst). Scale bar is 100 µm. **(E)** In vitro glucose-induced insulin secretion by iβ-like cell spheroids. Data are calculated as mean ± SEM for 3 independent experiments, 1-3 replicates per experiment. *, P< 0.05; **, P< 0.01; ***, P< 0.001 relative to 2D in C using one-sample test, or between indicated conditions in B and E using unpaired t-test.

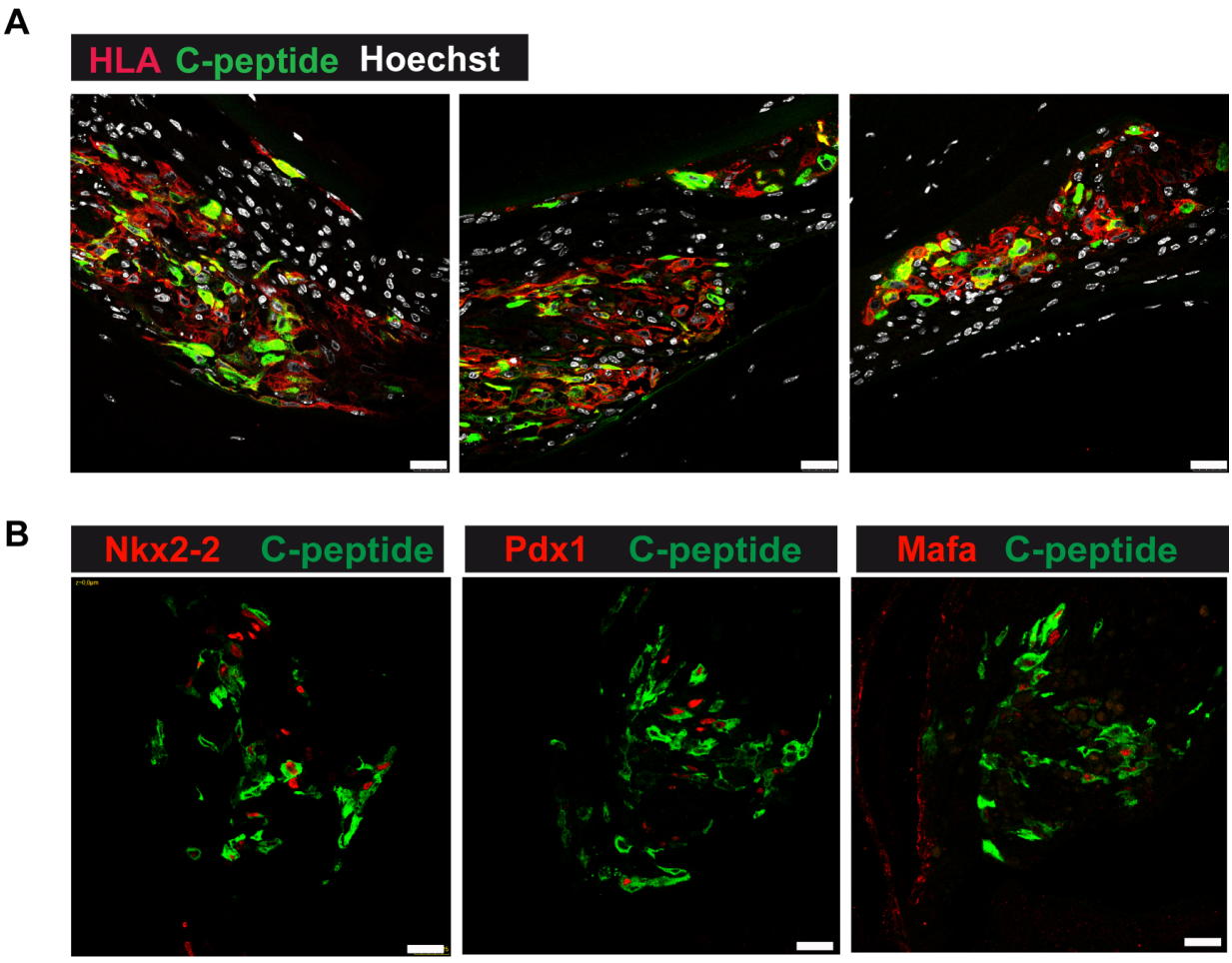

Supplementary S5: Immunostaining of iβ-cell spheroids ten days after their transplantation into the anterior chamber of the eye of NSG mice. Representative immunofluorescence images showing **(A)** C-peptide staining (green), HLA (red) and cell nuclei marked with Hoechst (white) and **(B)** C-peptide (green) with the indicated transcription factors (red). Scale bars are 25 µm.

Table S1. Comparison of gene expression levels between iβ-cells maintained in 2D culture, iβ-cell spheroids (3D) and human islets for the indicated genes. Fold expression values are calculated using qPCR data presented in Figures 1D&E, 2A, 3A-C and 5C.

Gene	Fold expression Islets/ iβ-cells 2D	Fold expression Islets/ iβ-cell 3D
ABCC8	2335	450
CHGB	23036	9251
CX36	3589	399
CXCR4	6	2
GIPR	10	6
GLP1R	163	100
INS	358	205
INSM1	134	41
KCNJ11	51	12
MAFB	8	4
NCAM1	2	2
NEUROD1	200	63
NEUROG3	2	3
NKX2-2	196	265
NKX6-1	117	37
PAX4	14	9
PAX6	425	327
PCSK1	16	5
PCSK2	81	48
PDX1	115	68
PTPRN (IA2)	30	25

Table S2. Comparison of circulating human insulin levels in transplanted mice between our study and several publications using stem cell-derived β-like cells.

Cells	**Number of cells**	**Site**	**Days post-transplantation**	**Insulin (μU/ml)**		**Source**
				basal	after glucose	
iβ-like cells	4 x 10^6	Subcutaneous	day 15	0.18-0.24	0.57-1.67	our study
			day 30	0-0.71	0.33-2.36	
iβ-like cells	4 x 10^6	omentum	day 15	0-0.63	0-5.24	our study
			day 30	0-5.2	2.36-5.23	
hES-derived endoderm	15 x 10^6	epididymal fat	day 94	13-36	56-110	Kroon et al. Nature Biotech 26, 443-452, 2008
hES-derived (PH, original differentation protocol)	5 x 10^6	kidney capsule	day 15	0-0.5	0-1	Pagliuca et al. Cell 159, 428-439, 2014
hES-derived SC-β cells (optimized protocol)	5 x 10^6	kidney capsule	day 15	1-5	1-11	
hiPSC-derived SC-β cells (optimized protocol)	5 x 10^6	kidney capsule	day 15	5	7.5	Millman et al. Nat Commun 7, 11463, 2016
hES-derived SC-β cells (optimized protocol)	5 x 10^6	kidney capsule	day 180	11	23	Velazco-Cruz et al. Stem cell Reports 12, 351-365, 2019

Table S3. List of oligonucleotides used for real time PCR.

Gene	Species	Primer ID	Primer sequence (5' to 3')
ABCC8	human	*Forward*	AGACCCTCATGAACCGACAG
ABCC8	human	*Reverse*	GGCTCTGTGGCTTTTCTCTC
ARX	human	*Forward*	GCAAGGAGGTGTGCTAAAGG
ARX	human	*Reverse*	GGAGTGTGCTGGTCCTCTGT
CD29	human	*Forward*	CAAAGGAACAGCAGAGAAGC
CD29	human	*Reverse*	ATTGAGTAAGACAGGTCCATAAGG
CD49a	human	*Forward*	GCTGGCTCCTCACTGTTGTT
CD49a	human	*Reverse*	CTCCATTTGGGTTGGTGACT
CHGB	human	*Reverse*	TTGGATGTCCTCCTCCCCTG
CHGB	human	*Forward*	CGCCAAGTCCTGAAGACGA
COL1A1	human	*Forward*	CTCGAGGTGGACACCACCCT
COL1A1	human	*Reverse*	CAGCTGGATGGCCACATCGG
CX36	human	*Forward*	GCAGCAGCACTCCACTATGA
CX36	human	*Reverse*	TACACCGTCTCCCCCACAAT
CXCL12	human	*Forward*	GAGCCAACGTCAAGCATCTC
CXCL12	human	*Reverse*	AGCTTCGGGTCAATGCACA
CXCR4	human	*Forward*	CGTCTCAGTGCCCTTTTGTTC
CXCR4	human	*Reverse*	CTGAAGTAGTGGGCTAAGGGC
FOXF2	human	*Forward*	CTACTTGCACCAGAACGCTC
FOXF2	human	*Reverse*	CGCAGGGCTTAATATCCTGACA
GCG	human	*Forward*	CACAGGGCACATTCACCAG
GCG	human	*Reverse*	TCTGGGAAATCTCGCCTTCC
GIPR	human	*Forward*	ACAATGTGAGAACCCAGAGAAG
GIPR	human	*Reverse*	CGCCTGAACAAACTCAAGATG
GLP1R	human	*Forward*	TTCTCTGCTCTGGTTATCGCC
GLP1R	human	*Reverse*	GGATGCAAACAGGTTCAGGT
HNF1B	human	*Forward*	ACCAAGCCGGTCTTCCATACT
HNF1B	human	*Reverse*	GGTGTGTCATAGTCGTCGCC
IGFBP4	human	*Forward*	TGTTGCACCATCTGCTTGGT
IGFBP4	human	*Reverse*	ATGTACCCCACCTCCCTAGC
INS	human	*Forward*	GCAGCCTTTGTGAACCAACA
INS	human	*Reverse*	TTCCCCGCACACTAGGTAGAGA
INSM1	human	*Forward*	TTTTGGAACCCCCACTTTTAC
INSM1	human	*Reverse*	CGAGACCAGACCGCATTT
KCNJ11	human	*Forward*	TGTGTCACCAGCATCCACTC
KCNJ11	human	*Reverse*	CACTTGGACCTCAATGGAGAA
LDHA	human	*Forward*	GCAAGAGGGAGAAAGCCGTC
LDHA	human	*Reverse*	CTTCCAAGCCACGTAGGTCA
LHX9	human	*Forward*	TGCCAAGGACGGTAGCATTT

LHX9	human	*Reverse*	GCAGCTCAGGTGGTAGACAG
MafA	mouse	*Forward*	CTTCAGCAAGGAGGAGGTCA
MafA	mouse	*Reverse*	TTGTACAGGTCCCGCTCTTT
MAFB	human	*Forward*	AACTTTGTCTTGGGGCACAC
MAFB	human	*Reverse*	GGGACCTCTCGGTTCTCTCT
MCT1 (SLC16A1)	human	*Forward*	CACCAGCGAAGTGTCATGGA
MCT1 (SLC16A1)	human	*Reverse*	ATCAAGCCACAGCCTGACAA
MYT1	human	*Forward*	AGTGTCTGCCCAGGTGTCTT
MYT1	human	*Reverse*	GACAGACAATAGCTGTGGGGA
NCAM 1	human	*Forward*	CCTCCCAGCCAGCAGATTAC
NCAM1	human	*Reverse*	CTCTCCAACGCTGATCTCCC
NEUROD1	human	*Forward*	AGGAAGAAGAGGAAGAGGAGGATG
NEUROD1	human	*Reverse*	TTGGTGGTGGGTTGGGATAAG
NEUROG3	human	*Forward*	AGACGACGCGAAGCTCACC
NEUROG3	human	*Reverse*	AAGCCAGACTGCCTGGGCT
Neurog3	mouse	*Forward*	CCCACCTAGCCCCACTCTCATACC
Neurog3	mouse	*Reverse*	CGCCGGCTTCTTCGCTGTTT
NKX2.2	human	*Forward*	CTTCTACGACAGCAGCGACAACCCG
NKX2.2	human	*Reverse*	CCTTGGAGAAAAGCACTCGCCGCTTT
NKX6-1	human	*Forward*	ACACGAGACCCACTTTTTCCG
NKX6-1	human	*Reverse*	GCCCCGCCAAGTATTTTGTT
OAT	human	*Forward*	CGTAAGTGGGGCTATACCGT
OAT	human	*Reverse*	CTGGTTGGGTCTGTGGAACT
P4H	human	*Forward*	TCGAGTTCACCGAGCAGACA
P4H	human	*Reverse*	GAACAGCAGGATGTGAGTCTTGA
PAX4	human	*Forward*	AGCAGAGGCACTGGAGAAAGAGTT
PAX4	human	*Reverse*	CAGCTGCATTTCCCACTTGAGCTT
PAX6	human	*Forward*	AGACACAGCCCTCACAAACA
PAX6	human	*Reverse*	ATCATAACTCCGCCCATTCA
PCSK1	human	*Forward*	AAGCAAACCCAAATCTCACCTGGC
PCSK1	human	*Reverse*	TCACCATCAAGCCTGCTCCATTCT
PCSK2	human	*Forward*	CCGGGTTCCTCTTCTGTGTC
PCSK2	human	*Reverse*	AGCAAAGGGAAGCTTTCGGA
PDGFRA	human	*Forward*	TGTGGGACATTCATTGCGGA
PDGFRA	human	*Reverse*	AAGCTGGCAGAGGATTAGGC
PDX1	human	*Forward*	CCCATGGATGAAGTCTACC
PDX1	human	*Reverse*	GTCCTCCTCCTTTTTCCAC
Pdx1	mouse	*Forward*	CCCCAGTTTACAAGCTCGCT
Pdx1	mouse	*Reverse*	CTCGGTTCCATTCGGGAAAGG
PRRX1	human	*Forward*	CGAGAGTGCAGGTGTGGTTT

PRRX1	human	*Reverse*	GAGCAGGACGAGGTACGATG
REST	human	*Forward*	CTCATACAGGAGAACGCCCA
REST	human	*Reverse*	GAGGCCACATAACTGCACTG
PTPRN (IA2)	human	*Reverse*	GGTGGAGGATGGTGTCAAGC
PTPRN (IA2)	human	*Forward*	AAGCTCCGCACCAGAAAGTC
SMAD3	human	*Forward*	CATCGAGCCCCAGAGCAATA
SMAD3	human	*Reverse*	TTTGGAGAACCTGCGTCCAT
SST	human	*Forward*	CAGTTTCTGCAGAAGTCCCTG
SST	human	*Reverse*	AATTCTTGCAGCCAGCTTTGC
TBP	human	*Forward*	ATCCCTCCCCCATGACTCCCATG
TBP	human	*Reverse*	ATGATTACCGCAGCAAACCGC
Tbp	mouse	*Forward*	ACCCTTCACCAATGACTCCTATG
Tbp	mouse	*Reverse*	ATGATGACTGCAGCAAATCGC
TBP	human(specific)	*Forward*	TGTGCTCACCCACCAACAAT
TBP	human(specific)	*Reverse*	ACGTCGTCTTCCTGAATCCC
TWIST2	human	*Forward*	CGCAAGTGGAATTGGGATGC
TWIST2	human	*Reverse*	CGATGTCACTGCTGTCCCTT

VIDEO CAPTIONS

Video S1

Video shows changes in fluorescence of an isolated iβ-like cell in response to high glucose (20mM) and high potassium (KCl 30mM). Cell had been pre-loaded with the calcium indicator Fluo-2. Video was recorded using a Leica TCS SPE confocal microscope with an incubation chamber set at 37°C, and a 40X oil immersion objective.

Video S2

Video shows fluorescence of parental fibroblasts HFF1 in response to high glucose (20mM) and high potassium (KCl 30mM). Cells had been pre-loaded with the calcium indicator Fluo-2. Note that fibroblasts exhibit no changes in fluorescence in response to the tested stimuli. Video was recorded using a Leica TCS SPE confocal microscope with an incubation chamber set at 37°C, and a 40X oil immersion objective.